Afforestation impact on soil temperature in regional climate model simulations over Europe

Giannis Sofiadis[1], Eleni Katragkou[1], Edouard L. Davin[2], Diana Rechid[3], Nathalie de Noblet-Ducoudre[4], Marcus Breil[5], Rita M. Cardoso[6], Peter Hoffmann[3], Lisa Jach[7], Ronny Meier[2], Priscilla Mooney[8], Pedro M.M. Soares[6], Susanna Strada[9], Merja H. Tolle[10], Kirsten Warrach Sagi[7]

[1]Department of Meteorology and Climatology, School of Geology, Aristotle University of Thessaloniki, Thessaloniki, Greece
[2]Department of Environmental Systems Science, ETH Zurich, Zurich, Switzerland
[3]Climate Service Centre Germany (GERICS), Helmholtz-Zentrum Geesthacht, Hamburg, Germany
[4]Laboratoire des Sciences du Climat et de l'Environnement; UMR CEA-CNRS-UVSQ, Université Paris-Saclay, Orme des Merisiers, bât 714, 91191 Gif-sur-Yvette CÉDEX, France.
[5]Institute of Meteorology and Climate Research, Karlsruche Institute of Technology, Karlsruche, Germany.
[6]Instituto Dom Luiz (IDL), Faculdade de Ciencias, Universidade de Lisboa, 1749-016 Lisboa, Portugal.
[7]Institute of Physics and Meteorology, University of Hohenheim, Stuttgart, Germany.
[8]NORCE Norwegian Research Centre AS/ Bjerknes Center for Climate Research, Bergen, Norway.
[9]International Center for Theoritical Physics (ICTP), Earth System Physics Section, Trieste, Italy.
[10]Universität Kassel, Center of Environmental Systems Research (CESR), Wilhelmshöher Allee 47, 34117 Kassel, Germany.

Correspondence to: Giannis Sofiadis (sofiadis@geo.auth.gr)

Abstract. In the context of the first phase of the Euro-CORDEX Flagship Plot Study (FPS) Land Use and Climate Across Scales (LUCAS), we investigate the afforestation impact on the seasonal cycle of soil temperature over the European continent with an ensemble of ten regional climate models (RCMs). For this purpose, each ensemble member performed two idealized land cover experiments in which Europe is covered either by forests or grasslands. The multi-model mean exhibits a reduction of the annual amplitude of soil temperature (AAST) over all European regions, although this not a robust feature among the models. In Mediterranean, the simulated AAST response to afforestation is between -4 K and +2 K while in Scandinavia the inter-model spread ranges from -7 K to +1 K. We then examine the role of changes in the annual amplitude of ground heat flux (AAGHF) and summer soil moisture content (SMC) in determining the effect of afforestation on AAST response. In contrast with the diverging results in AAST, all the models consistently indicate a widespread AAGHF decrease and summer SMC decline due to afforestation. The AAGHF changes effectively explain the largest part of the inter-model variance in AAST response in most regions, while the changes in summer SMC determine the sign of AAST response within a group of three simulations sharing the same land surface model. Finally, we pair FLUXNET sites to compare the simulated results with observation-based evidence of the impact of forest on soil temperature. In line with models, observations indicate a summer ground cooling in forested areas compared to open lands. The vast majority of models agree with the sign of the observed reduction in AAST, although with a large variation in the magnitude of changes. Overall, we aspire to emphasize the effects of afforestation on soil temperature profile with this study, given that changes in the seasonal cycle of

Geoscientific
Model Development
Discussions

35   soil temperature potentially perturb crucial biochemical processes. Such perturbations can be of societal relevance as
afforestation is proposed as a climate change mitigation strategy.

1 Introduction

There is currently a strong policy focus on afforestation as a possible greenhouse gases (GHG) mitigation strategy to meet
ambitious climate targets (Grassi et al., 2017). However, understanding the full climate consequences of the large-scale
40   deployment of such a strategy requires to consider also the biophysical effects of afforestation arising from changes in
evapotranspiration efficiency, surface roughness and surface albedo (Betts, 2000; Bonan, 2008; Davin and de Noblet-
Ducoudre, 2010; Perugini et al., 2017; Duveiller et al., 2018).

Previous studies have attempted to quantify the biophysical impact of land-use changes (LUC) on global scale, employing
either an ensemble of global climate model (GCM) simulations (Pitman et al., 2009; Noblet-Ducoudré et al., 2012; Boisier et
45   al., 2012; Lejeune et al., 2018) or applying a single GCM individually (Claussen et al., 2001; Davin et al., 2007; Li et al.,
2016). (Davin and de Noblet-Ducoudre, 2010) analysed a GCM's sensitivity to idealized global deforestation, indicating that
the net biophysical impact results from the balance between radiative and non-radiative processes. Over the tropical zone,
deforestation induced a warming owing to a reduction in evapotranspiration rate and surface roughness. On contrary,
deforestation resulted in a cooling over the temperate and boreal zones, because an albedo increase provided the dominant
50   influence in these regions. In the context of Land-Use and Climate, IDentification of Robust Impacts (LUCID) model inter-
comparison project, (Noblet-Ducoudré et al., 2012) diagnosed the LUC effects over North America and Eurasia between the
present and the pre-industrial era. They found that deforestation caused a systematic surface albedo increase across all
seasons, leading to a reduction in available energy accompanied by a decrease in the sum of turbulent fluxes. Furthermore,
(Lejeune et al., 2018) using a suite of simulations from Coupled Model Inter-comparison Project Phase 5 (CMIP5)
55   concluded that moderate deforestation over Eurasia and North America has substantially led to a local warming of present-
day hot extremes since pre-industrial time.

Regional climate models (RCMs) have been also used individually to address the LUC effects on regional scale (Gálos et al.,
2013; Tölle et al., 2018; Cherubini et al., 2018; Belušić et al., 2019). (Lejeune et al., 2015) used a state-of-the-art RCM to
explore the biophysical impacts of possible future deforestation on Amazonian climate. They demonstrated that the projected
60   land cover changes for 2100 could slightly increase the mean annual surface temperature by 0.5 °C and decrease the mean
annual rainfall by -0.17 mm/day compared to present conditions. (Strandberg and Kjellström, 2019) performed regional
climate simulations undertaking scenarios of maximum deforestation/reforestation over Europe using a single RCM. They
concluded that total deforestation could result in a warmer summer by 0.5 °C - 2.5 °C in Europe, while the effect on
precipitation was less certain.

65   The crucial need to better constrain and represent the LUC biophysical forcing in regional climate simulations over Europe,
generated the Euro-CORDEX (Jacob et al., 2020) FPS Land Use and Climate Across Scales (LUCAS) initiative (Davin et

al., 2020) which operates under the auspices of the World Climate Research Program (WCRP). In the first phase of LUCAS, for first time multi-model and multi-physics simulations were performed under a common experimental protocol to address the RCMs sensitivity to extreme land use changes in Europe. The first experiment assumed a maximum forest coverage while the second a maximum grass coverage over Europe.

Contrasting these two idealized LUC experiments, (Davin et al., 2020) analysed the robustness of RCMs responses to afforestation and according to their results, afforestation implied an albedo-induced warming over northern Europe during winter and spring. Furthermore, the summer near-surface temperature response to afforestation was subject to large uncertainty, strongly related with disagreement among models in land-atmosphere interactions. Analysing a part of RCM ensemble established within LUCAS FPS, (Breil et al., 2020) examined the impact of afforestation on the diurnal temperature cycle in summer. Their results revealed that afforestation dampened the diurnal surface temperature cycle, while the opposite was true for the temperature in the lowest atmospheric model level.

The responses of atmospheric processes to afforestation have been extensively discussed in previous studies. However, the changes in soil temperature profile following the afforestation remain unexplored up to now in LUCAS community. (MacDougall and Beltrami, 2017) suggested that deforestation may has led to a long-term warming of the ground, associated with a reduction of heat fluxes towards the atmosphere. Here, we investigate the impact of afforestation on soil temperature across Europe, as simulated by a suite of ten RCMs established within the frame of the first phase of LUCAS FPS. The comparison between two extreme LUC scenarios, representing the Europe entirely covered by forest and grass respectively, enable us to gain insights into the impacts of theoretical afforestation on soil temperature variations (Sect. 3.1). Taking into account the second heat conduction law, we examine both the annual amplitude of ground heat flux (AAGHF) (Sect. 3.2) and summer soil moisture content (SMC) (Sect. 3.3) responses to afforestation, in order to explain the inter-model spread in annual amplitude of soil temperature (AAST) (Sect. 3.4). In addition, we compare the simulated impact on AAST with observational evidence based on FLUXNET paired sites, classified as forest or open land (Sect. 3.5).

2 Data and Methods

2.1 Regional Climate Model ensemble

Two idealized LUC experiments are carried out using an ensemble of ten RCMs. **Table 1** provides a brief description of the RCM ensemble characteristics, while more information about the land and atmospheric setups can be found in (Davin et al., 2020). Compared to (Davin et al., 2020) the current model ensemble includes simulations from two additional RCMs (CCLM-CLM5.0 and WRFc-NoahMP) while one of the RCMs (RCA) is not included here because the necessary variables for the analysis were missing. Compared to CCLM-CLM4.5, CCLM-CLM5.0 is coupled with a modified version of CLM 5.0 (Lawrence et al., 2019) that includes biomass heat storage (Swenson et al., 2019; Meier et al., 2019). WRFc-NoahMP shares the same land component as WRFb-NoahMP but differs in the atmospheric set-up. Namely, WRFc-NoahMP used the Yonsei University (YSU) scheme (Hong et al., 2006) as planetary boundary layer (PBL) parameterization

and MM5 as surface layer scheme. In addition, new simulations were carried out for WRFb-NoahMP and WRFb-CLM4.0 to

100 address minor bug fixes.

Table 1: Characteristics of the RCMs participating in the study. JLU – Justus-Liebig-Universität Gießen; BTU: Brandenburgische Technische Universität; KIT – Karlsruhe Institute of Technology; ETH – Eidgenössische Technische Hochschule Zürich; SMHI – Swedish Meteorological and Hydrological Institute; ICTP – International Centre for Theoretical Physics; GERICS – Climate Service Center Germany; IDL – Instituto Amaro Da Costa;

105 **UHOH – University of Hohenheim; BCCR – Bjerknes Center for Climate Research; AUTH – Aristotle University of Thessaloniki. The full table including the parameterization schemes and settings used, can be found in (Davin et al., 2020).**

Model name	Institute	RCM version	LSM	Soil column
CCLM-TERRA	JLU/BTU	COSMO_5.0_clm9	TERRA-ML	10 layers down to 15.3 m. First 9 (8) layers are thermally (hydrologically) active.
CCLM-VEG3D	KIT	COSMO_5.0_clm9	VEG3D (Breil et al., 2018)	10 layers down to 15 m. First 9 (8) layers are thermally (hydrologically) active.
CCLM-CLM4.5	ETH	COSMO_5.0_clm9	CLM4.5 (Oleson et al., 2013)	15 thermally active layers down to 42 m. The first 10 layers are hydrologically active.
CCLM-CLM5.0	ETH	COSMO_5.0_clm9	CLM5.0 (Lawrence et al., 2019)	25 thermally active layers down to 50 m. The first 20 layers are hydrologically active.
RegCM-CLM4.5	ICTP	RegCMv4.6.1	CLM4.5 (Oleson et al., 2013)	15 thermally active layers down to 42 m. The first 10 layers are hydrologically active.
REMO-iMOVE	GERICS	REMO2009	iMOVE (Wilhelm et al., 2014)	5 thermally active layers down to 9.8 m. One water bucket.
WRFa-NoahMP	IDL	WRFv3.8.1	NoahMP	4 layers down to 2 m.
WRFb-NoahMP	UHOH	WRFv3.8.1	NoahMP	4 layers down to 2 m.
WRFc-NoahMP	BCCR	WRFv3.8.1	NoahMP	4 layers down to 2 m.
WRFb-CLM4.0	AUTH	WRFv3.8.1	CLM4.0 (Oleson et al., 2010)	10 thermally and hydrologically active layers down to 3.43 m.

2.2 Experimental design

In LUCAS, each participating RCM undertook two different simulations, applying the same experimental design. In the first

110 experiment, called FOREST, models are forced with a vegetation map representing a Europe fully covered by trees, where they can realistically grow. Bare lands, urban areas and water bodies were conserved as in original model maps. In the second experiment, called GRASS, the models integrate the same vegetation map, with the only difference that trees are entirely replaced by grasslands. Detailed description about the creation of these maps and the way they are implemented into

the respective RCMs can be found in (Davin et al., 2020). All simulations are performed over the Euro-CORDEX domain

115 (Jacob et al., 2020) with a spatial resolution of 0.44º (~50 km), forced by ERA-Interim reanalysis data (Dee et al., 2011). Our analysis covers the 30-year period 1986-2015 and focuses on the following eight European sub-regions as described in (Christensen and Christensen, 2007): Alps (AL), British Isles (BI), Eastern Europe (EA), France (FR), Iberian Peninsula (IP), Mediterranean (MD), Mid-Europe (ME) and Scandinavia (SC) (**Figure S1**).

We consider the FOREST minus GRASS differences, implying the impact of theoretical maximum afforestation on soil

120 temperature in Europe. The second heat conduction law is widely used by LSMs to update temperature in each soil layer (Eq. 1):

$$\frac{dT}{dt} = \frac{d}{dz}[k * \frac{dT}{dz}]$$

where k is thermal diffusivity (m^2 s^{-1}) defined at the layer node depth z (m), t is time (s) and $\frac{dT}{dz}$ is the spatial gradient of temperature (K m^{-1}) in the vertical direction z (m).

125 The spatial gradient of soil temperature is strongly linked with the ground heat flux (GHF) quantity, while the thermal diffusivity is a function of soil texture and moisture. Since soil texture remains unchanged in our experiments, soil moisture is the only variable which influence the thermal diffusivity. Particularly, changes in soil moisture alter the heat capacity of soil column and consequently affect the soil temperature variations. In the present analysis, GHF is calculated as the residual of surface energy balance because the actual GHF outputs were not available in most models. A main caveat of this approach

130 constitutes the fact that when the soil is decoupled from the upper atmospheric boundary layer (eg snow covered ground), the residual of surface energy balance does not represent the energy exchange on soil surface but the energy budget on the atmosphere-snow interface**.**

2.3 FLUXNET observational data

We use measured or high-quality gap-filled data of soil temperature on monthly scale from the FLUXNET2015 Tier 2

135 dataset to complement the model-based analysis. Detailed documentation on data and processing methods can be found in (Pastorello et al., 2020).

In order to extract the potential effect of afforestation from observations, we employ a space-for-time analogy by searching for pairs of neighbouring flux towers located over forest (deciduous, evergreen or mixed trees) and open land (grasslands or croplands), respectively. This approach has been used in previous studies aiming to investigate biophysical impacts of local

140 LUC and evaluate LSM performance (Broucke et al., 2015; Chen et al., 2018). In search for site pairs, the following criteria were defined: the two sites have to 1) be located in the Euro-CORDEX domain, 2) differ in the type of vegetation, one site being forested and the other one being either cropland or grassland, 3) have a linear distance within the horizontal resolution of the performed simulations (less than 50 km), 4) have a common measurement period of at least two years, and 5) provide measurements at common depth below the ground surface. In total, we found 14 sites that met our criteria and combined in

145 ten pairs. Their locations are depicted in **Figure 1** and their characteristics are reported in **Table 2**. The median linear

distance between the paired sites is 11.4 km and their median elevation difference is 125 m.
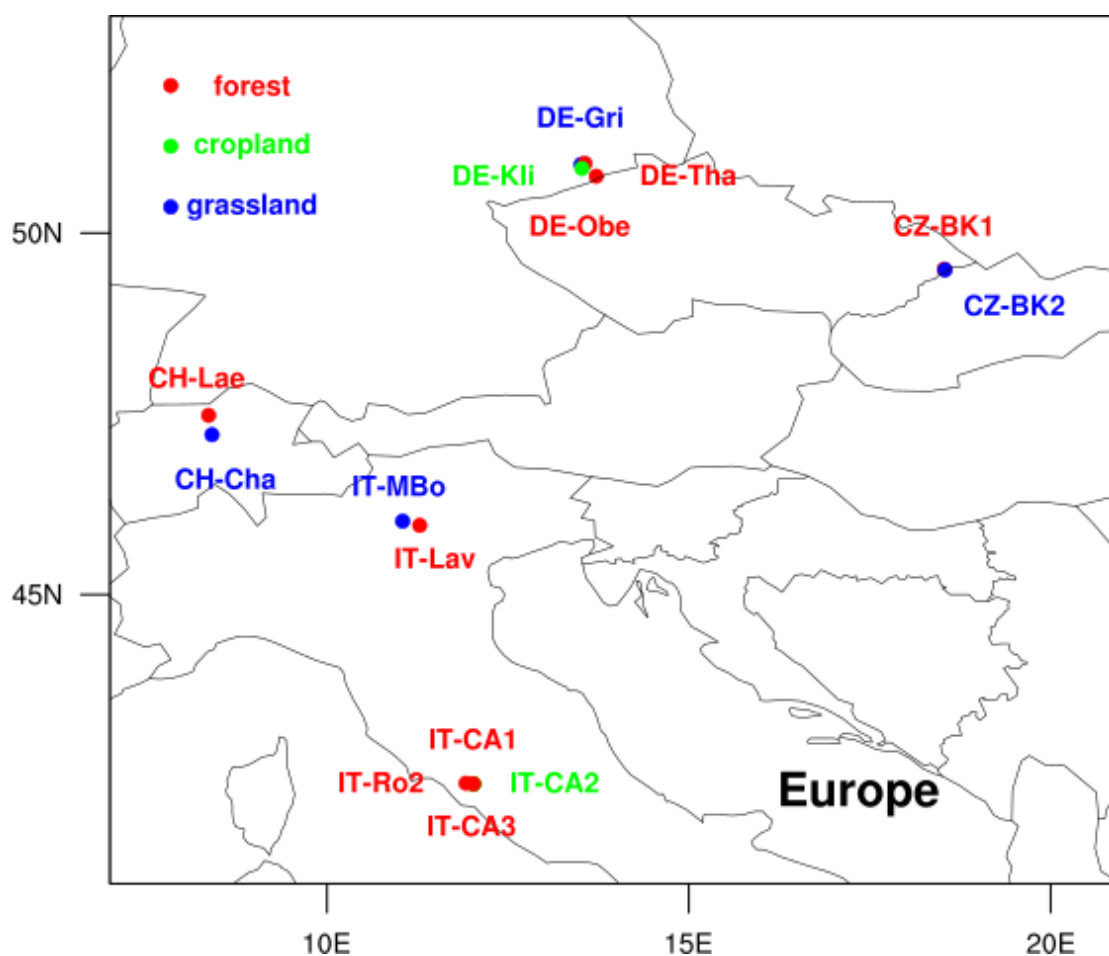
Figure 1: Location of the sites selected from FLUXNET2015 dataset.

150 **Table 2: Characteristics of the sites selected from FLUXNET2015 dataset. DBF – Deciduous Broadleaf Forest; ENF – Evergreen Needleleaf Forest; MF – Mixed Forest; CRO – cropland; GRA – grassland, as described by the International Geosphere-Biosphere Programme (IGBP) classification scheme.**

Pair ID	FLUXNET site ID	(Latitude, Longitude)	Elevation (m)	Land cover type	Distance (km)	Time period	Measurement depth
1	IT-CA1	(42.380,12.026)	200	DBF	0.3	2011-2014	15cm
	IT-CA2	(42.377,12.026)	200	CRO			
2	IT-CA3	(42.380,12.022)	197	DBF	0.4	2011-	15cm

Geoscientific
Model Development
Discussions

	IT-CA2	(42.377,12.026)	200	CRO		2014	
3	IT-Ro2	(42.390,11.920)	160	DBF	8.7	2011-2012	15cm
	IT-CA2	(42.377,12.026)	200	CRO			
4	CZ-BK1	(49.502,18.536)	875	ENF	0.9	2004-2012	5cm
	CZ-BK2	(49.494,18.542)	855	GRA			
5	DE-Tha	(50.962,13.565)	385	ENF	4.1	2004-2014	10cm
	DE-Gri	(50.950,13.512)	385	GRA			
6	DE-Obe	(50.786,13.721)	734	ENF	23.4	2008-2014	10cm
	DE-Gri	(50.950,13.512)	385	GRA			
7	DE-Tha	(50.962,13.565)	385	ENF	8.4	2004-2014	10cm
	DE-Kli	(50.893,13.522)	478	CRO			
8	DE-Obe	(50.786,13.721)	734	ENF	18.4	2008-2014	10cm
	DE-Kli	(50.893,13.522)	478	CRO			
9	IT-Lav	(45.956,11.281)	1353	ENF	19.3	2003-2013	10cm
	IT-Mbo	(46.014,11.045)	1550	GRA			
10	CH-Lae	(47.478,8.364)	689	MF	30	2005-2014	10cm
	CH-Cha	(47.210,8.41)	393	GRA			

The close proximity between the flux towers of paired sites ensures almost similar atmospheric conditions, so that
155 differences can be primarily attributed to the different vegetation cover. Applying a simple linear correlation test, the differences either in elevation or separation between the flux towers of paired sites are not the dominant factors in determining the changes in AAST ($r = -0.2$ and $r = -0.3$, respectively).

For comparison with the RCMs, we consider the observed mean monthly soil temperature differences (forest minus open land) averaged over all paired sites. This is then compared with the mean of the grid cells matching the locations of the
160 observational pairs in the various RCMs (FOREST minus GRASS). Modelled soil temperature was linearly interpolated to the common measurement depth that is available for each pair site and averaged over the time period 2003-2014 which covers the observational time span.

Last but not least, the observational setup does not fully resemble the experimental design applied in RCM ensemble. The spatial scale of afforestation applied in models is significantly different from the small forest patches the flux towers are
165 located in. The extreme afforestation in RCMs has the potential to triggers atmospheric feedbacks which strongly modify the local and regional climate, whereas such feedbacks are not realistic in observations.

3. Results

3.1 Soil temperature response

Figure 2 shows the afforestation (FOREST minus GRASS) effect on the annual amplitude of soil temperature (AAST) at 1
170   meter below the ground surface. AAST is calculated as the difference between the warmest and the coldest month of an
average year (based on the 1986-2015 climatology), implying that the maximum and minimum value may occur in different
months depending on regions.

A large range of AAST response is simulated across RCMs. Six out of the ten simulations show a decrease in the AAST due
to afforestation in most regions (**Figure S2**). Four out of these six ensemble members employ a version (4.0, 4.5 and 5.0) of
175   the CLM land surface model (LSM), coupled with a different atmospheric model (CCLM, RegCM or WRF). Therefore, it
can be assumed that, the agreement in sign of changes between these simulations resides to a great extent in the choice of a
similar LSM. Also, the latter finding holds true for three out of ten ensemble members exhibiting the opposite behaviour,
namely an increase in AAST. These three members utilize the NoahMP LSM coupled to different WRF atmospheric model
configurations (WRFa, WRFb and WRFc); WRFa shows the most intense and systematic changes in AAST with
180   afforestation (close to 2 K in several regions), while the other two configurations (WRFb and WRFc) show changes less than
1 K. The weakest response is simulated by REMO-iMOVE with temperature changes ranging from -0.5 K in southern
Europe to +0.5 K in Scandinavia.

It is worth noting that the differences between simulations with the same atmospheric model (WRFb) coupled to different
LSMs (NoahMP and CLM) disagree in sign of changes, especially over southern Europe. This finding suggests again that
185   the choice of the LSM drives in a great extent the sign of changes in AAST (increase/decrease), while the choice of the
atmospheric model further modulates (dampens/enhances) the magnitude of the signal. Another sub-ensemble is built around
the CCLM atmospheric model participating with three different LSMs (TERRA, VEG3D, CLM version 4.5 and 5.0)
illustrating diverse results; CCLM-TERRA exhibits the strongest decrease in AAST with maximum changes exceeding -4 K
over many regions. The CCLM-CLM configurations provide similar responses with maximum changes up to -2 K. The
190   CCLM-VEG3D exhibits a distinct behaviour with small AAST increases over central Europe.
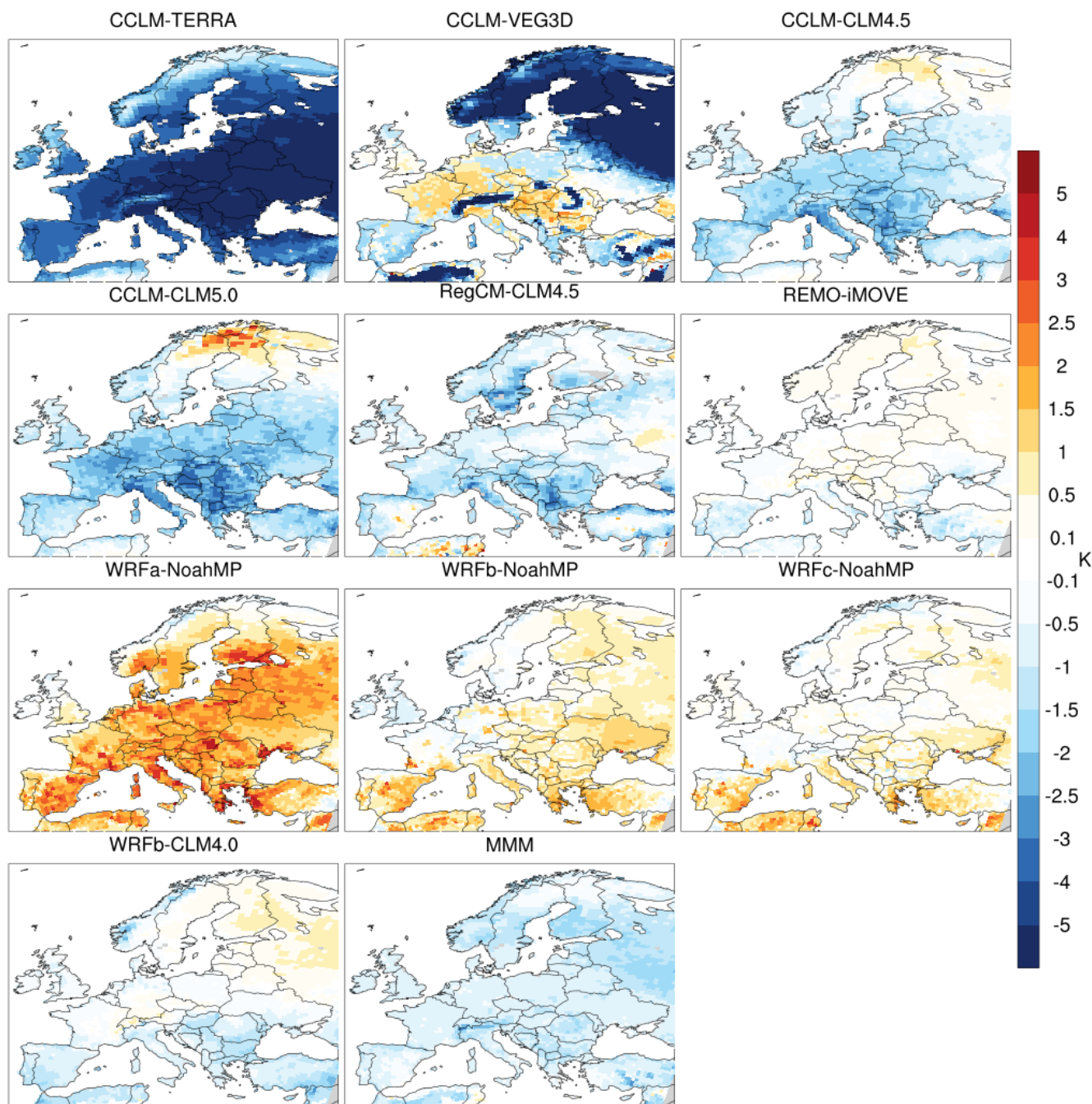
Figure 2: Afforestation (FOREST minus GRASS) impact on the annual amplitude of soil temperature (AAST) at 1 meter depth. MMM: Multi-Model-Mean.

To better understand the changes in AAST, we examine the annual cycles of soil temperature for both experiments, FOREST

195 (red) and GRASS (blue) over two European sub-regions, the Mediterranean (**Figure 3**) and Scandinavia (**Figure 4**). These

two regions are selected as they are representative of southern and northern Europe, respectively, while similar figures can be found for all European subregions in the supplementary material (**Figures S3-S8**). Moreover, in **Figures S9-S16** we present the afforestation effect on mean monthly soil temperature within the top 1 meter of the soil over all the regions for each modelling system.

200   Over the Mediterranean region almost all models respond to afforestation, with REMO-iMOVE exhibiting the lowest sensitivity to the land cover change forcing in all seasons. From the remaining simulations, six out of the nine show that summer (maximum) soil temperatures are higher in the GRASS than in the FOREST experiment. All simulations included in this category involve the CLM (coupled with CCLM, RegCM, WRF), TERRA and the VEG3D LSMs. The winter (minimum) soil temperatures in the same modelling systems do not differ for the two experiments (FOREST and GRASS)

205   and thus we can attribute the decrease in AAST, discussed before, exclusively to the summertime climate processes over the Mediterranean region. The three remaining simulations of the ensemble show the opposite behaviour, with higher forest soil temperatures in summer and they all involve the NoahMP LSM. Similar to the first group of simulations, the winter soil temperature sensitivity to afforestation is pretty small, and as a result the AAST in WRF-NoahMP modelling systems has a positive sign of change.

210   In Scandinavia, considerable disagreement in the model behaviours is visible, as three members show a clear decrease in summer soil temperature similar to the Mediterranean area (CCLM-TERRA, CCLM-VEG3D, RegCM-CLM4.5), two models exhibit the opposite behaviour with increased soil temperature (CCLM-CLM5.0, WRFa-NoahMP) and the rest modelling systems appear not to be sensitive to afforestation across the seasons. Obviously, the response of the modelling systems is mostly based on the selection of the LSM; the CCLM model coupled to TERRA, VEG3D and CLM provides

215   totally different results, with the CCLM-VEG3D being the most responsive (up to -7 K) to afforestation during the summer. In winter, the soil temperature differences due to afforestation are small and with a tendency for increase. As seen in **Figure 4**, the simulated response exhibits great variability during the summer season, when models disagree both on the sign and magnitude of changes.
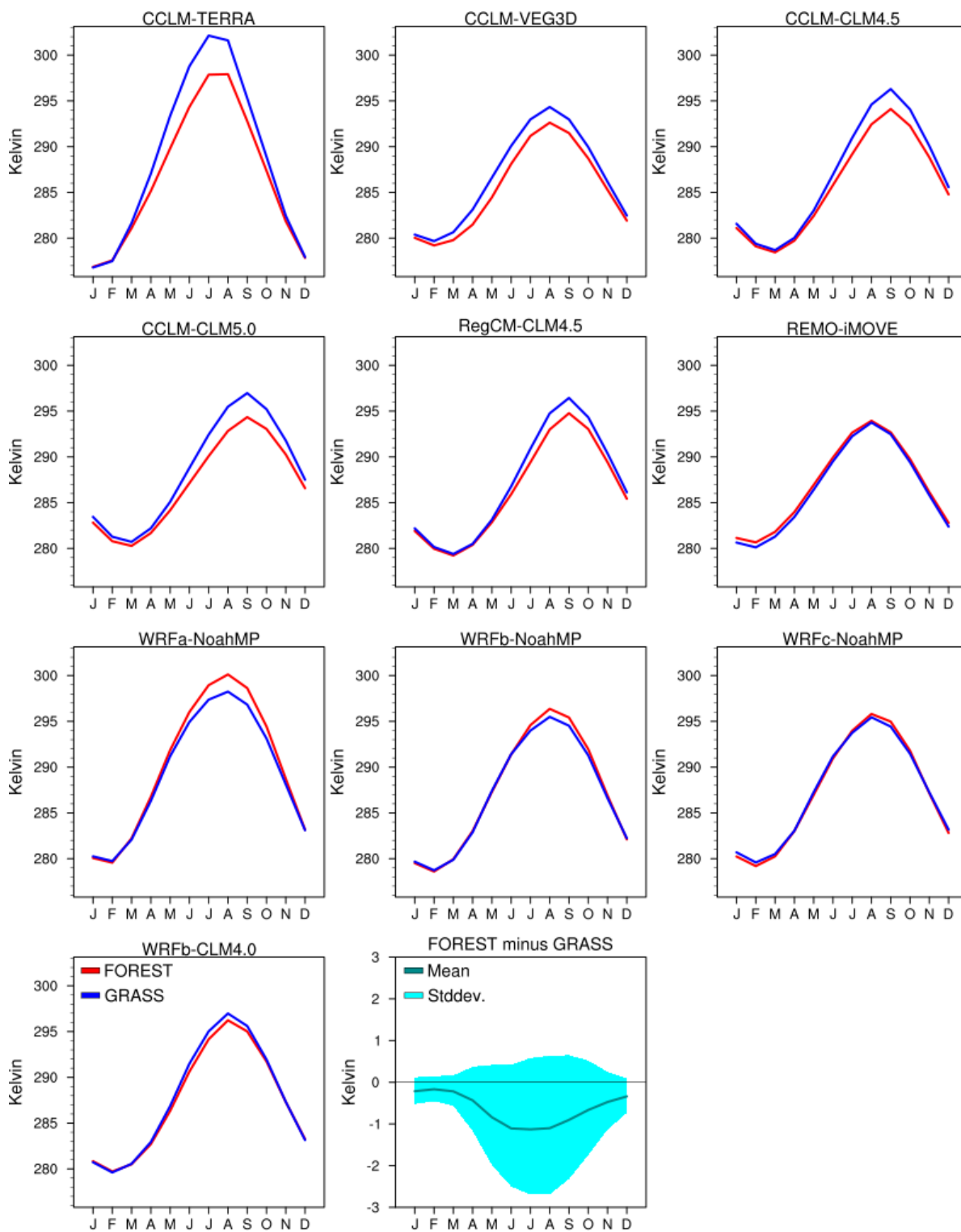
Figure 3: Annual soil temperature cycle for FOREST and GRASS over Mediterranean.
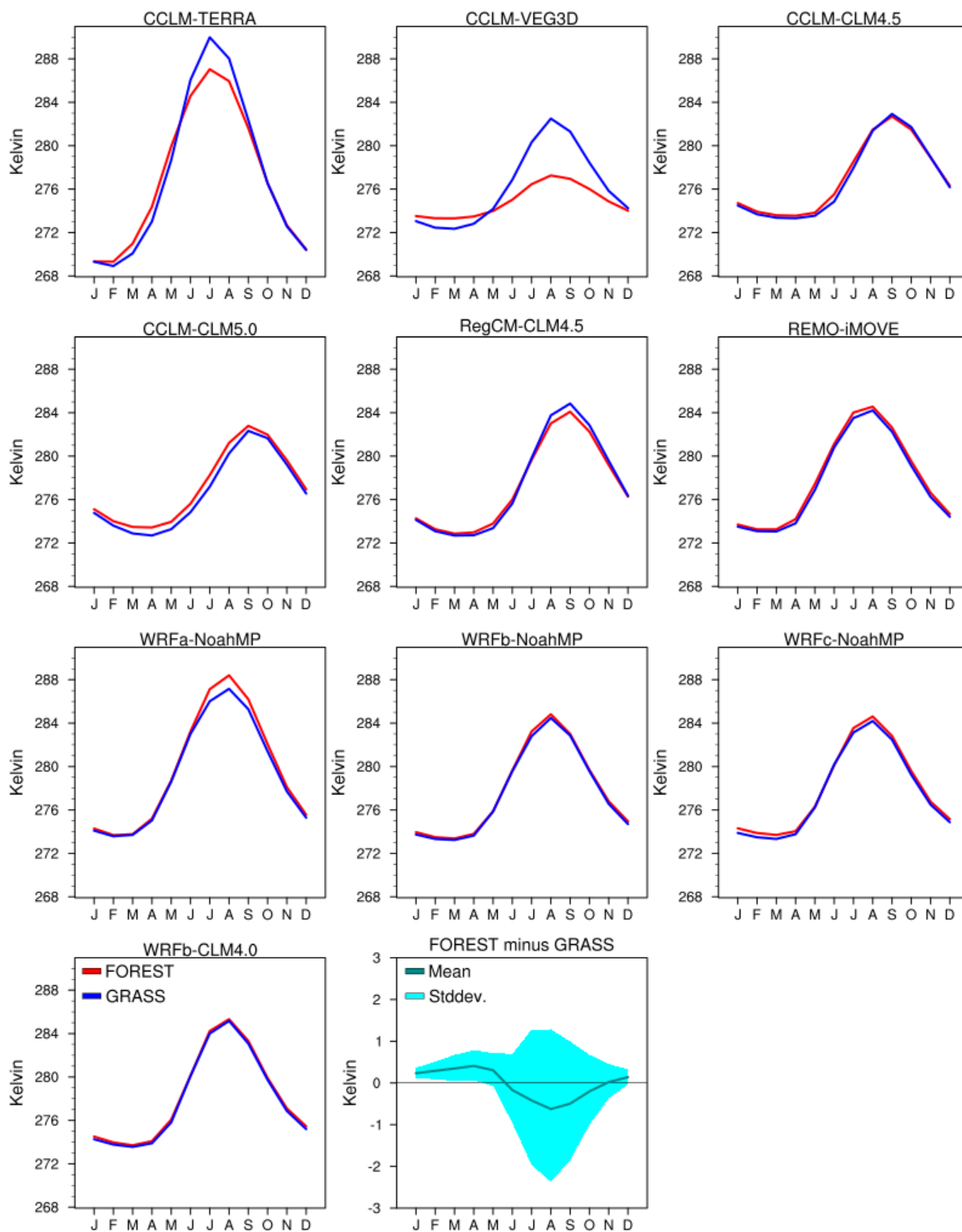
Figure 4: Annual soil temperature cycle for FOREST and GRASS over Scandinavia.

3.2 Annual amplitude of GHF

225   In this section, we focus on the annual amplitude of GHF (AAGHF) as a potential driver for the AAST response to afforestation. Taking into account the second heat conduction law, a larger (smaller) AAGHF could result in a larger (smaller) AAST, when considering equal soil moisture conditions between the two experiments.

Figure 5 shows maps of the afforestation impact on the AAGHF in Europe. In contrast to the diverse simulated response in AAST, all the ensemble members consistently show a reduction in AAGHF due to afforestation in all European subregions

230   (**Figure S17**). Scandinavia appears to be the most sensitive among the regions, where four out of the ten ensemble members show a reduction in AAGHF greater than -10 W/m^2. The WRF-NoahMP modelling systems together with REMO-iMOVE show small AAGHF changes compared to the rest of the models, especially over the central and southern Europe. The choice of LSM affects the magnitude of changes in AAGHF; different scales of AAGHF decrease are observed between the members sharing the CCLM atmospheric model, especially between CCLM-VEG3D and CCLM-TERRA. Also, in central

235   Europe several grid-cells in CCLM-VEG3D exhibit the opposite behaviour, namely a small AAGHF increase.
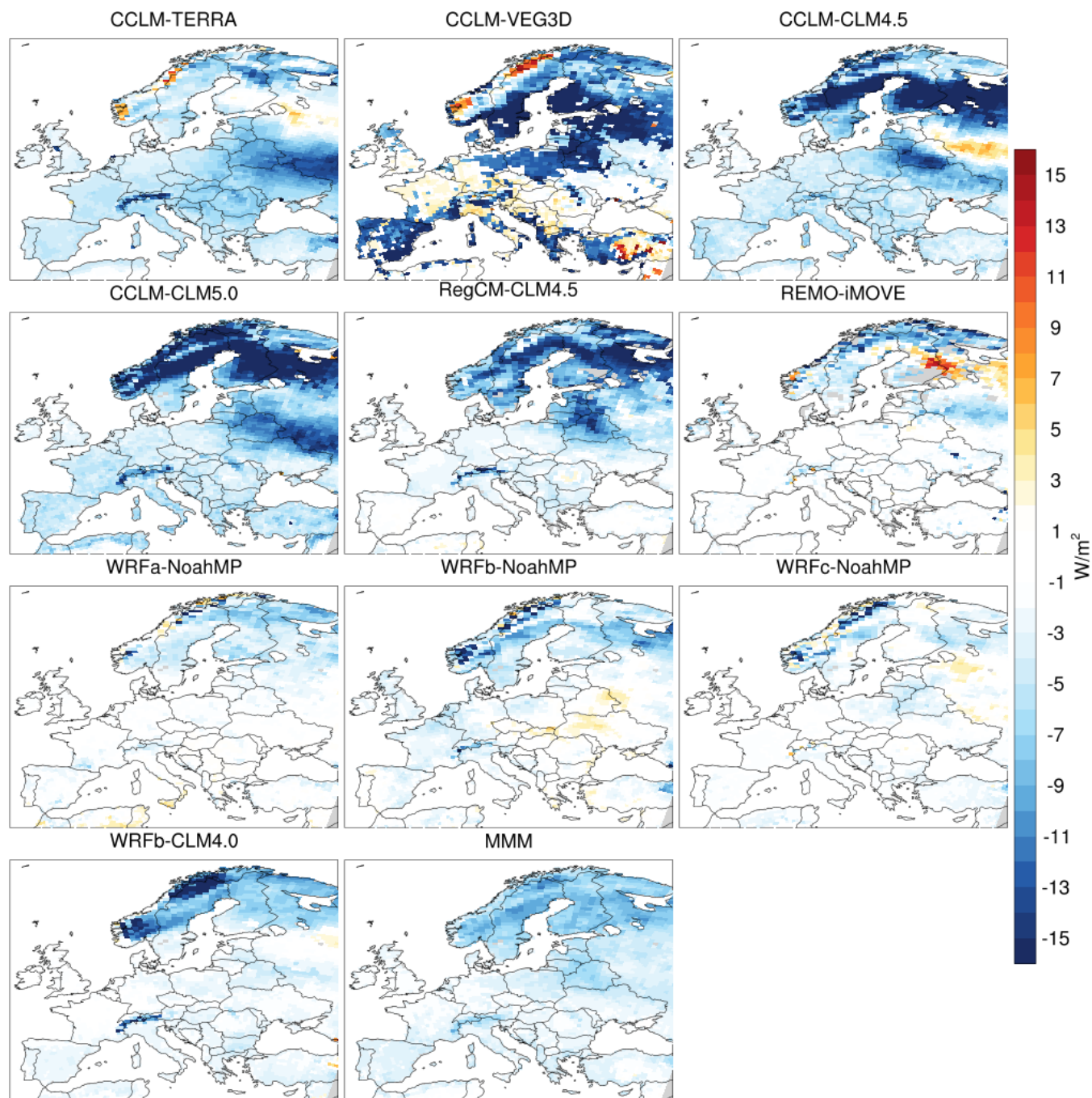
Figure 5: Afforestation (FOREST minus GRASS) impact on annual amplitude of ground heat flux (AAGHF). MMM:Multi-Model-Mean.

To further understand the AAGHF response, we examine the annual GHF cycles for both experiments, FOREST (red) and
240   GRASS (blue) over the Mediterranean (**Figure 6**) and Scandinavia (**Figure 7**). Similar figures can be found for the rest
European subregions in the supplementary material (**Figure S18-S23**).

Over the Mediterranean region, RegCM-CLM4.5 together with the sub-ensemble around the CCLM model show seasonal
contrasts in the GHF response to afforestation. Specifically, larger GHF values are found for GRASS during the spring and
summer seasons, whereas the GHF is larger for FOREST during the autumn and winter seasons. The switch from NoahMP
245   to CLM4.0 in WRFb atmospheric configuration alters the pattern of GHF changes; WRFb-NoahMP shows low sensitivity to
afforestation with small increase during the summer, while WRFb-CLM4.0 exhibits a GHF decrease during the warm
months. The remaining modelling systems show minor GHF changes throughout the year.

Over Scandinavia, all RCMs except WRF-NoahMP modelling systems, present seasonal contrasts in GHF changes similar to
Mediterranean area; larger GHF values for GRASS during summer, but larger GHF for FOREST during autumn, winter and
250   spring. The dampening of the annual GHF cycle over Scandinavia is a robust feature among the models, although is not
reflected in the mixed AAST response, where the models produce a large spread in summer soil temperature due to
afforestation as reported in previous section.

The GHF in WRF-NoahMP modelling systems exhibits low sensitivity to afforestation in both regions. The small decrease
in AAGHF, originated from small GHF differences during spring, is not consistent with the AAST increase in these
255   simulations. Thus, the changes in AAGHF could not be considered responsible for the AAST response in simulations with
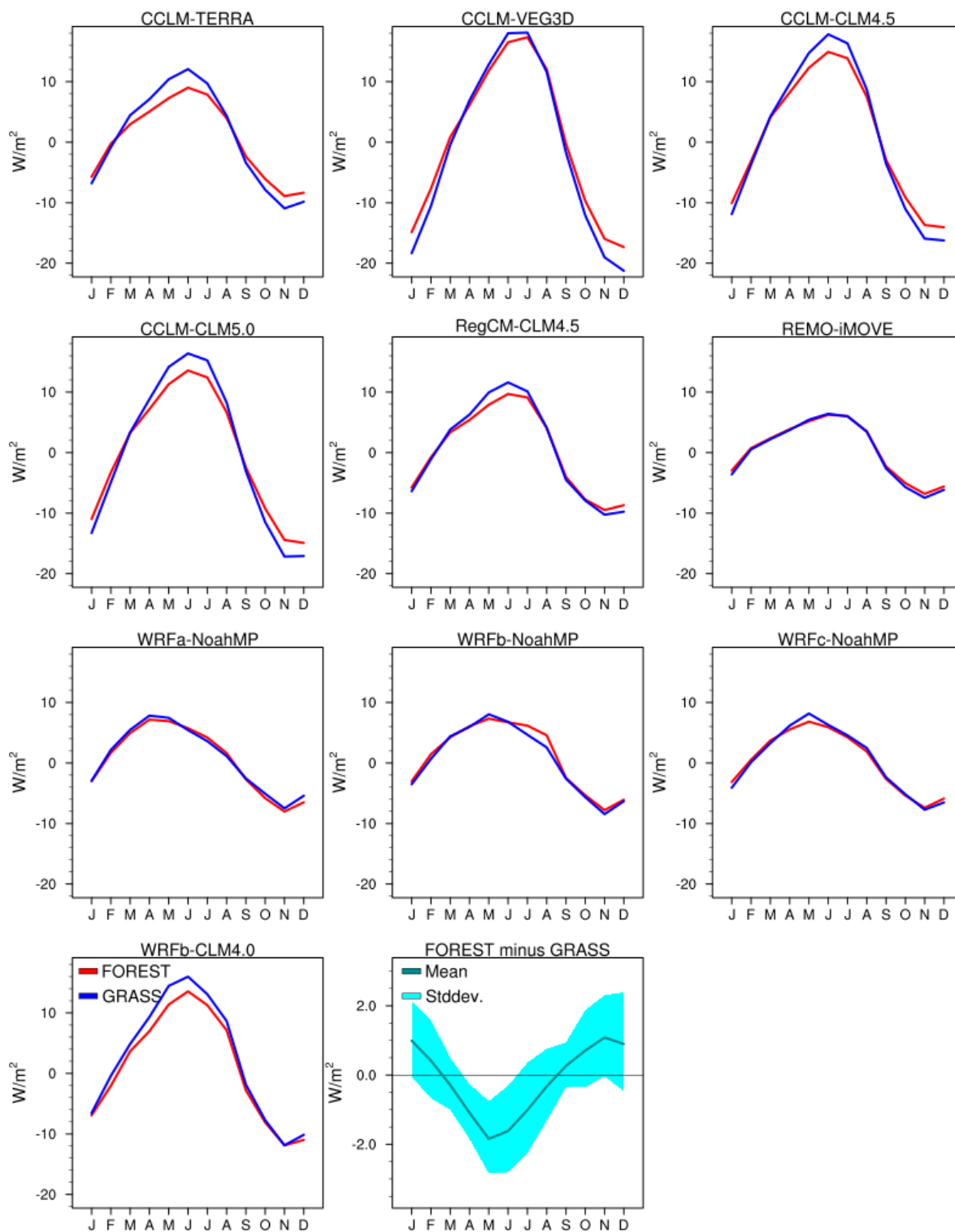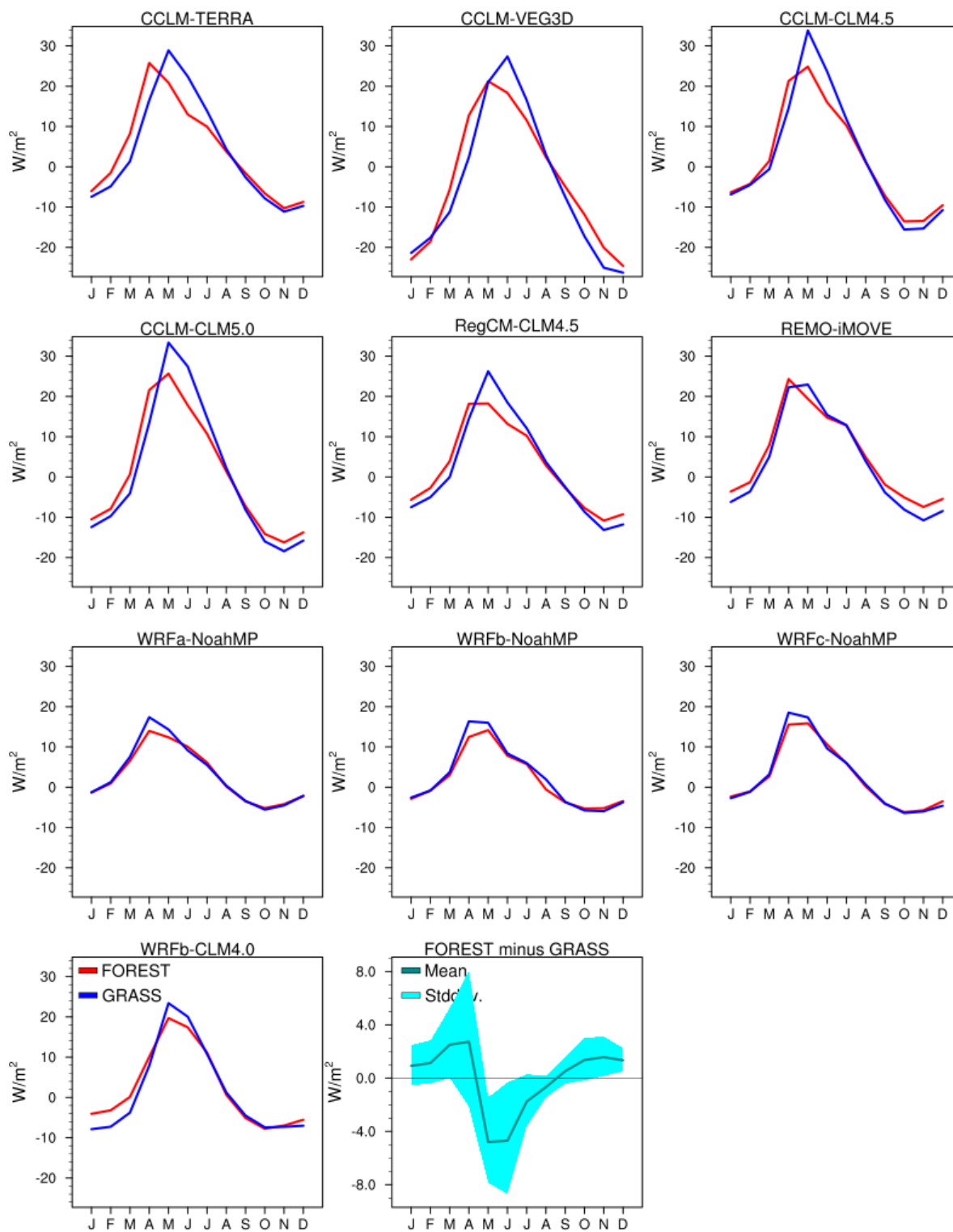NoahMP.

**Figure 6: Annual GHF cycle for FOREST and GRASS over Mediterranean.**

**Figure 7: Annual GHF cycle for FOREST and GRASS over Scandinavia.**

In **Figure 8** and **Figure 9** we show the year-round changes in surface fluxes over Mediterranean and Scandinavia regions, in order to discuss the underlying processes behind the dampening of the annual GHF cycle with afforestation. Similar figures can be found for the rest European subregions in the supplementary material (**Figures S24-S29**).

Over both regions, all the ensemble members exhibit a widespread increase in net radiation during the autumn and winter,
265   which is a direct consequence of the decreased surface albedo with afforestation. This increase in net radiation leads to larger GHF values with afforestation during these seasons. In spring and summer, the increase in net radiation is even more pronounced since the incoming solar radiation becomes greater over the northern hemisphere during these seasons. Especially over Scandinavia during spring, the net radiation is sharply increased because of the snow masking effect of trees. However, the increased available radiative energy with afforestation is accompanied by a systematic increase in the sum of
270   turbulent fluxes. This is attributed to high surface roughness which characterize the forested areas and enhance the heat exchange in soil-vegetation-atmosphere continuum (Breil et al., 2020). In most simulations the afforestation-induced increase in the sum of turbulent fluxes overcompensate the radiative energy gain during the warm months. Thus, GHF is smaller with afforestation during spring and summer over the Mediterranean region. For Scandinavia, this holds true only for summer, since the enhanced turbulent heat fluxes are not strong enough to offset the large increase in net radiation during
275   spring. The seasonal pattern of GHF changes is not reproduced by REMO-iMOVE over Mediterranean and the sub-ensemble around NoahMP. REMO-iMOVE shows small changes in surface fluxes which is probably attributed to the low albedo sensitivity to afforestation across the seasons in its simulations. The modelling systems with NoahMP exhibit strong increase in net radiation especially during summer, may related to the reduced cloud cover with afforestation in these simulations (Breil et al., 2020). The seasonal contrast in GHF changes is not illustrated in WRF-NoahMP modelling systems,
280   since the enhanced heat fluxes are almost equal with the increased radiative energy in most months.
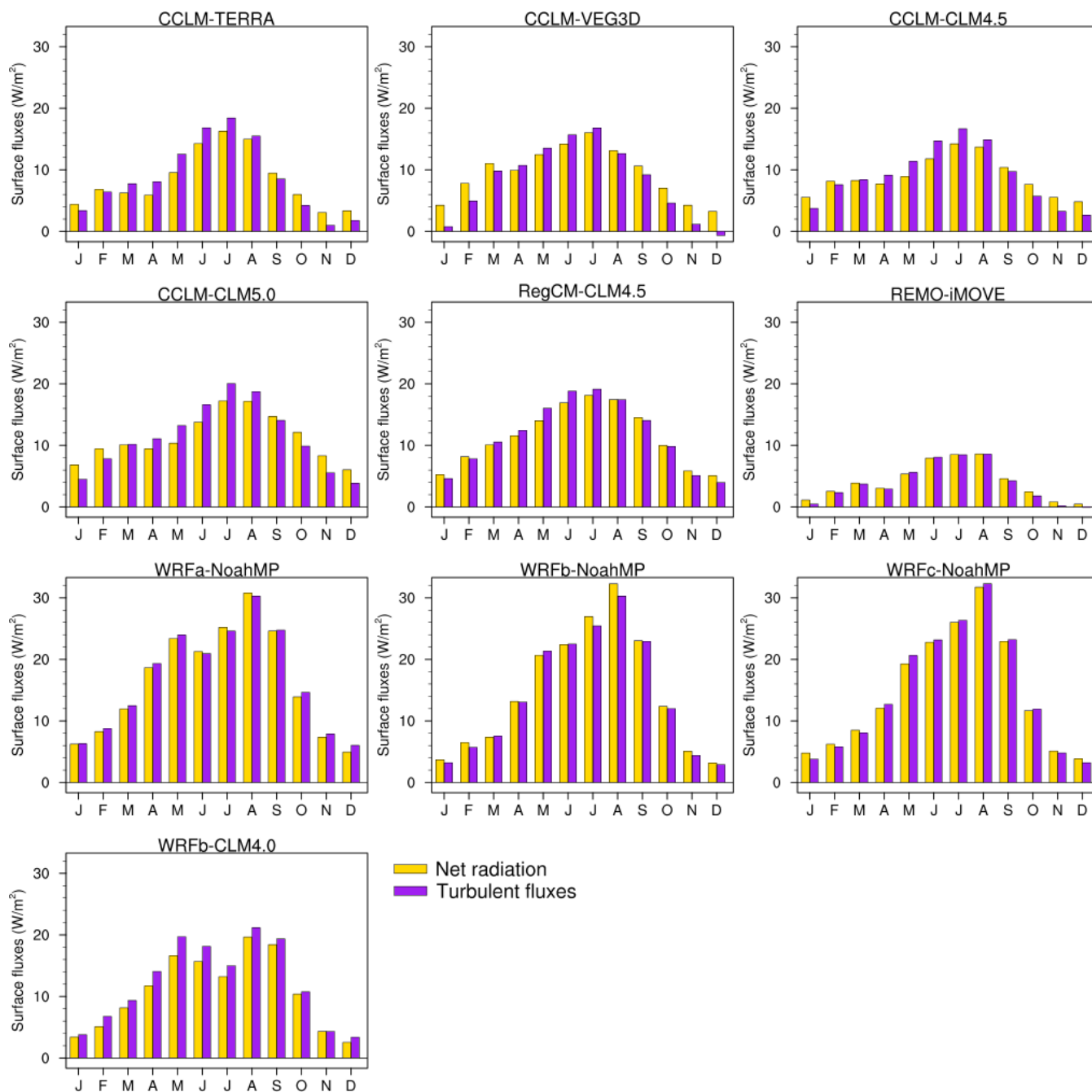
Figure 8: Mean monthly changes in net radiation and turbulent fluxes due to afforestation (FOREST minus GRASS) over Mediterranean. Turbulent fluxes are defined as the sum of sensible and latent heat fluxes.
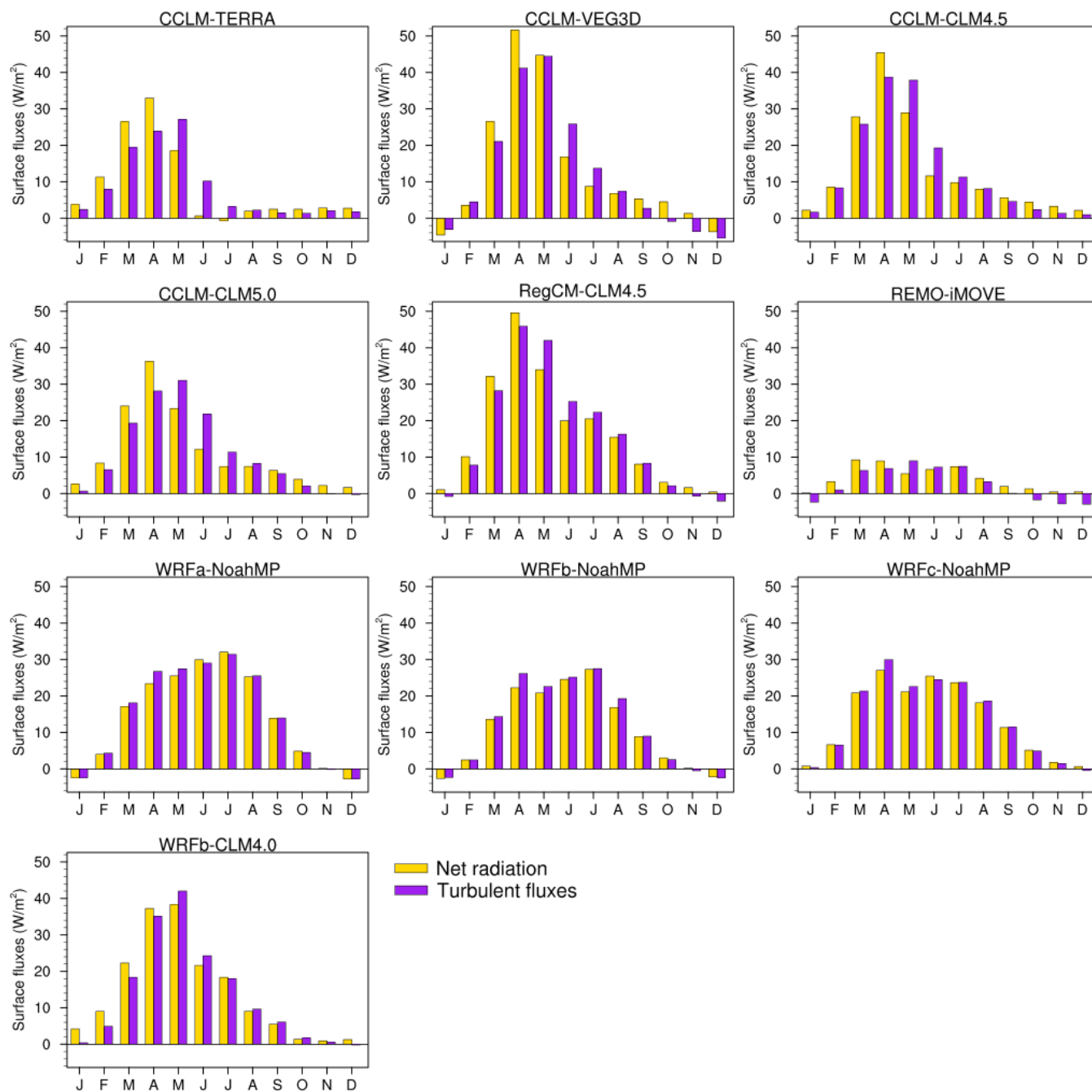
Figure 9: Mean monthly changes in net radiation and turbulent fluxes due to afforestation (FOREST minus GRASS) over Scandinavia. Turbulent fluxes are defined as the sum of sensible and latent heat fluxes.

3.3 Soil moisture

In addition to GHF, thermal diffusivity is also a parameter involved in the equation of the second heat conduction law and is
290 linked with the temporal soil temperature variations. Soil moisture strongly regulates the thermal diffusivity within the soil
column, since affecting the heat capacity of soil layers. It is expected that a drier (wetter) soil column would lead to a larger
(smaller) AAST owing to its smaller(larger) heat capacity, when considering equal soil heat fluxes between the two
experiments.

In **Figure 10** we map the mean summer differences in soil moisture content (SMC) in the top 1 meter of the soil over the
295 domain of interest (FOREST minus GRASS). A widespread soil moisture decrease is simulated over the biggest part of the
domain, although with considerable variation in the magnitude of changes among the models. The choice of LSM produces a
large spread of responses; within the sub-ensemble around CCLM the SMC change ranges from small decrease in CCLM-
CLM4.5 and CCLM-CLM5.0 to more than -30 kg/m^2 for CCLM-TERRA in several regions (**Figure S30**). Differences in the
magnitude of changes are also present between the WRFb-NoahMP and WRFb-CLM4.0. The atmospheric processes also
300 affect the magnitude of afforestation effect on SMC; among the modelling systems sharing NoahMP, WRFa-NoahMP
appears to be the most responsive, with changes exceeding -20 kg/m^2 in southern Europe. Further, many grid-cells over
central and northern Europe exhibit SMC increase in WRFb-NoahMP and WRFc-NoahMP configurations, in contradiction
with the extensive soil moisture reduction in WRFa-NoahMP.

Geoscientific
Model Development
Discussions
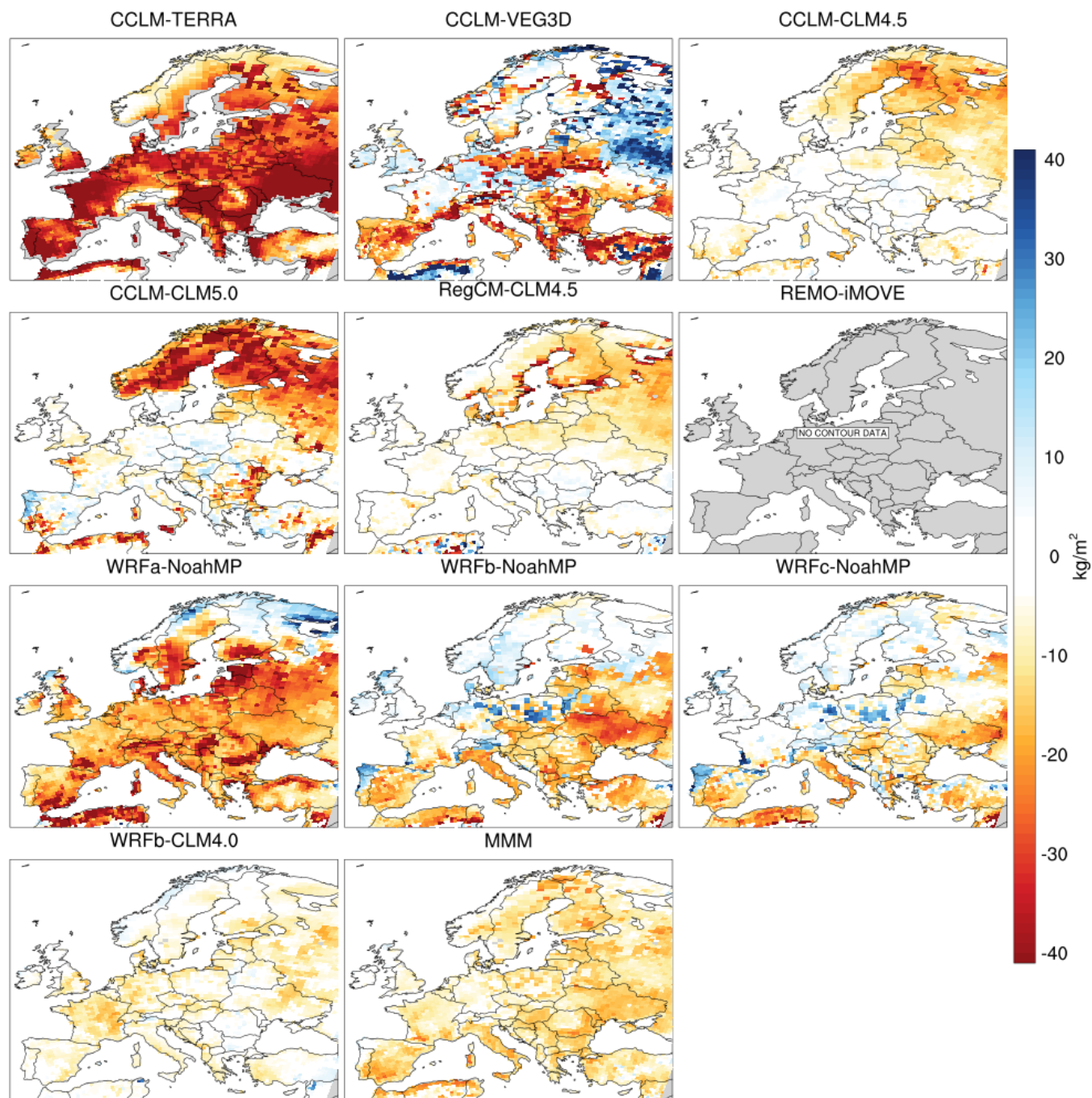
305 **Figure 10: Afforestation (FOREST minus GRASS) impact on soil moisture content (kg m⁻²) of the top 1 meter of the soil during summer. REMO-iMOVE is not included because it employed a bucket scheme for soil hydrology in the LUCAS Phase 1 experiments, which does not allow a separation of soil moisture into different layers.**

The surface water balance (P-E), defined as the difference between precipitation (P) and total evapotranspiration (E), decreases with afforestation during summer in the majority of models over the whole Europe (**Figure S31**). In most

310   simulations, the decrease in the terrestrial water budget originates from increased evapotranspiration rates with afforestation. In summer, high LAI values do not allow solar radiation to reach the ground surface, as a result soil evaporation is limited and transpiration dominates overall evapotranspiration. Specific characteristics, such as the big leaf area, the deep roots, the great available energy due to low albedo and the mixing of the upper atmospheric boundary layer because of the high surface roughness, enhance the transpiration rate in forests. Although, CCLM-VEG3D and WRFa-NoahMP show positive sign of

315   changes in water balance in regions of central and southern Europe, owing to decreased evapotranspiration with afforestation. This is probably linked with low atmospheric demands for hydrates in FOREST experiment of CCLM-VEG3D. In WRFa-NoahMP, the use of Grell-Freitas as convection scheme, exploits the transpiration facilitating features of forests causing extreme soil drying from very early in summer. Therefore, the evapotranspiration rate lowers with afforestation, because the dry soil is not able to satisfy the atmospheric needs for hydrates.

320   The soil moisture changes with depth would indirectly reveal the afforestation effect on the evapotranspiration process during summer. The water uptake for transpiration occurs in different depths within the soil column for grasslands and forests. In grasslands, the soil water needed for transpiration is extracted from shallow layers, because the large fraction of their roots is located there, depleting the moisture of upper soil. On the other hand, forests have a deeper root distribution, thus consuming water from a bigger soil water reservoir. In **Figure 11** we show the afforestation-induced soil moisture

325   changes within the top 1 meter of the soil over Mediterranean and Scandinavia. Similar plots for the other sub-regions can be found in **Figure S32** of the supplementary material. The heterogeneity of SMC changes with depth is evident in most models, especially in Mediterranean. In Scandinavia, distinct drying of the uppermost soil layers is shown by some models, especially CCLM-CLM4.5 and CCLM-CLM5.0, which is related to changes in water amounts from snow melt. The different structures of land models and the various descriptions of physiological characteristics of plants in LSMs, such as the root

330   distributions, differentiate the pattern of SMC changes with depth among the simulations. Also, possible biases in the representation of surface fluxes potentially affect the afforestation effect on soil moisture. For example, in CCLM-TERRA the latent heat fluxes are strongly increased with afforestation, as discussed in previous studies (Davin et al., 2020; Breil et al., 2020), inducing intense drying of the soil column.
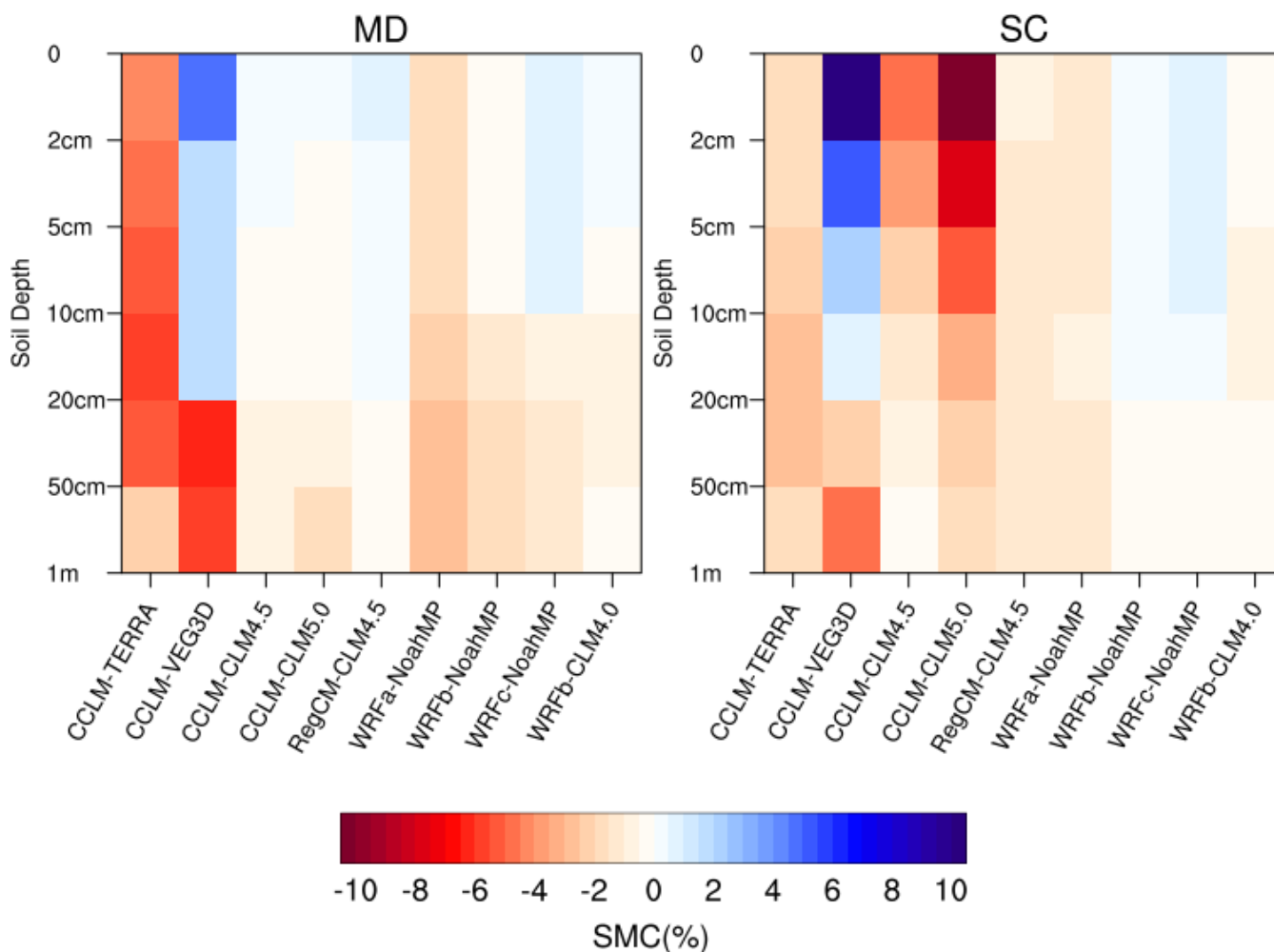
Figure 11: Summer changes in soil moisture content (SMC) due to afforestation (FOREST minus GRASS) in the top 1 meter of the soil over Mediterranean (MD) and Scandinavia (SC).

3.4 Attributing the inter-model spread in AAST to AAGHF and SMC

With the aim to quantify the effect of AAGHF response and summer SMC changes on AAST response to afforestation, we conduct a linear regression analysis including the respective simulated responses over all the European sub-regions. Particularly, we use the changes in AAGHF and summer SMC as explanatory (independent) variables, to determine to what extent they influence the changes in AAST (dependent variable). When we regress both the explanatory variables against the AAST response, we find that the coefficient of multiple determination (R^2) is above 74% in most regions (**Figure 12**). The AAGHF response is the dominating factor which largely predicts the inter-model variance in AAST in most regions. On the other hand, the predictive ability of the summer SMC changes is not strong, with a small contribution to the explanation of the inter-spread in AAST over many regions of central Europe. In Scandinavia, the statistical approach shows low effectiveness in predicting the inter-model variance in AAST response. This is probably related to the fact that the ground in

Scandinavia is usually snow-covered in several months of year, thus the use of the residual of surface energy balance, as a proxy for the actual GHF output, is not suitable for describing the energy exchange on soil-atmosphere interface. Other variables, such as the changes in snow amount, could contribute to the explanation of AAST response in this region. Another

350   caveat of the statistical approach constitutes the interaction between the changes in SMC and the impact of AAGHF changes on AAST response. The relatively drier soil conditions with afforestation reduce the heat capacity of soil column, and as a result attenuate the effect of AAGHF decrease on soil temperature. This interaction effect reduces the predictive ability of AAGHF response as explanatory variable.

Another question arises from our results is why the WRF-NoahMP modelling systems exhibit a positive sign of changes in

355   AAST, while simulating a decrease in AAGHF with afforestation in line with the other simulations. The AAGHF sensitivity to afforestation is low in these simulations, because the radiative energy gain due to lower forest albedo is almost equal to the increased surface heat fluxes owing to higher forest surface roughness. The AAGHF decrease results from small GHF reduction during spring. Although, afforestation causes drier soil conditions during summer, which lead to smaller soil heat capacity. As a consequence, WRF-NoahMP members exhibit higher soil temperatures with afforestation in summer season

360   and consequently larger annual soil temperature cycle, in contradiction to the majority of modelling systems where the AAGHF response mainly determines the AAST changes.
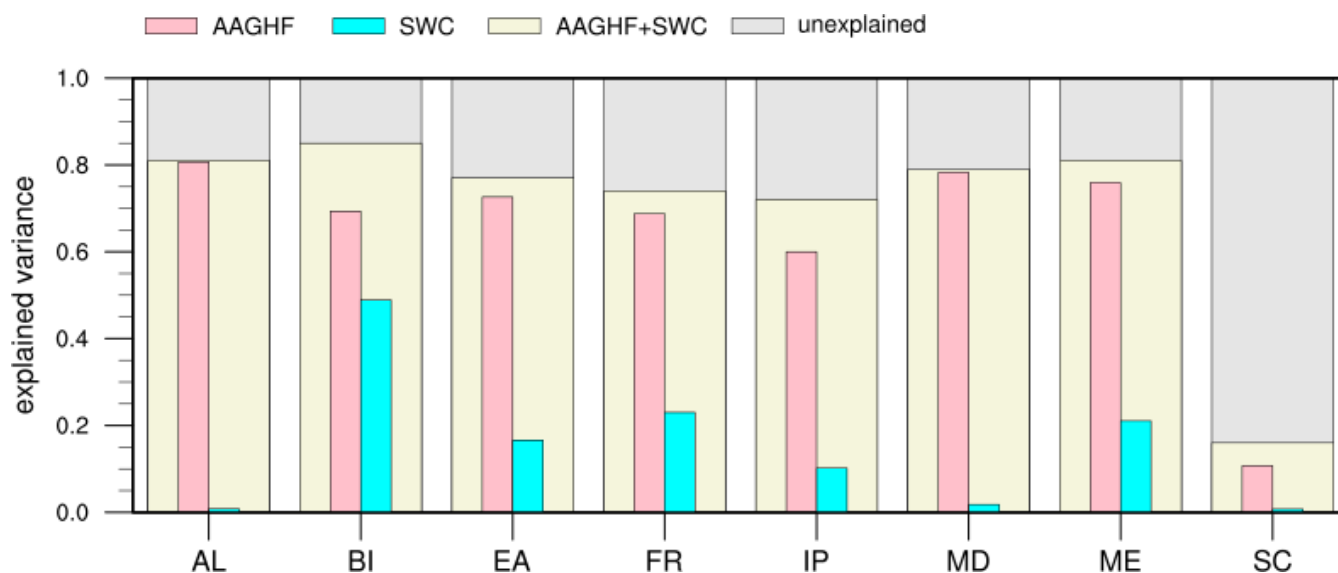

Figure 12: The fraction of inter-model variance in AAST response (FOREST minus GRASS) explained by changes in

365   **AAGHF, soil moisture content (SMC) or both combined (AAGHF+SMC). Bars represent the coefficient of determination (R^2) values derived from linear regression analysis applied over each sub-region.**

3.5 FLUXNET paired sites

In this section, we compare the simulated impact on AAST with observational evidence of afforestation effect on soil temperature, based on ten FLUXNET paired sites. In winter, simulations and observations illustrate insignificant changes in
370 soil temperature with afforestation (**Figure 13**). Although, the magnitude of afforestation effect in the observations is amplified during summer, revealing a strong cooling up to -3 K. The majority of models captures the seasonal pattern of changes in soil temperature and particularly the observed summer cooling, albeit with considerable variation in the magnitude of changes. CCLM-TERRA shows the largest changes in summer soil temperature (-5 K), whereas WRFb-NoahMP and WRFc-NoahMP exhibit subtle summer cooling smaller than -1 K. On the other hand, WRFa-NoahMP, CCLM-
375 VEG3D and REMO-iMOVE do not capture the observed signal of changes in summer, simulating a warming. Especially REMO-iMOVE shows a yearly warming, opposite to the observed cooling throughout the year. According to the observations, afforestation dampens the mean annual soil temperature range by almost -3 K which is qualitatively consistent with most RCMs, in which the decrease ranges from -5 K for CCLM-TERRA to -0.2 K for REMO-iMOVE. Notable exception is WRFa-NoahMP which exhibits a distinct increase greater than 1 K, in contradiction with the observational
380 evidence. Within the sub-ensemble of CCLM model, the selection of CLM (4.5 or 5.0) as the land component, refines the simulated impact of afforestation on AAST. Also, between the simulations sharing the same WRF atmospheric configuration (WRFb), the selection of CLM4.0 against NoahMP improves the representation of soil temperature response to afforestation.

26
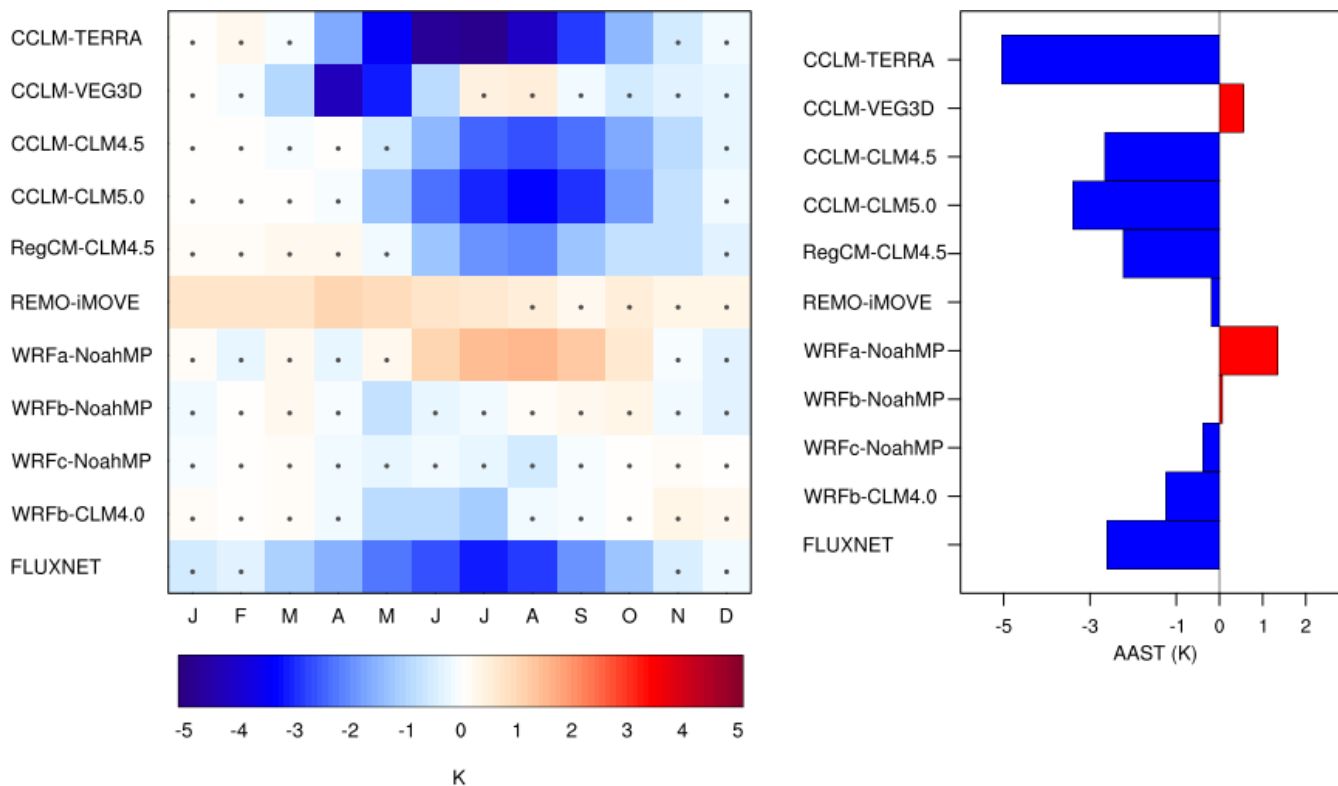
Figure 13: Left: Observed and simulated impact of afforestation on mean monthly soil temperature. The dots indicate the differences which are insignificantly different from zero in a two-sided t-test at 95% confidence level. Right: The changes in AAST(K) due to afforestation across models and observations. The observational differences are averaged over all the paired FLUXNET sites (forest minus open land) and the simulated changes are averaged over the corresponding model grids (FOREST minus GRASS).

4. Conclusions

In this study, we employed the experimental design established within LUCAS FPS, to investigate the afforestation impact on soil temperature over the Euro-CORDEX domain. Particularly, two idealized land cover change experiments performed by an ensemble of ten RCMs, in which the European land surface is represented as fully covered by forest and grass, respectively. The majority of simulations showed a dampening of the annual soil temperature cycle with afforestation, owing to changes in summer soil temperature. A large inter-model spread produced, ranging from -7 K to +2 K depending on model and region.

The dampening of the annual GHF cycle largely explained the inter-model variance in AAST response to afforestation in most regions. The AAGHF decrease was a robust feature among the models. An increase of the net shortwave radiation, owing to the lower forest albedo, induced higher GHF in winter. On the other hand, the enhanced surface heat fluxes in

summer, owing to large surface roughness of forested areas, offset the radiative energy gain induced by the albedo effect,
400   resulting in a decrease in summer GHF.

Previous studies which addressed the effects of LUC on soil temperature have reported similar results with the present work. (Ni et al., 2019) conducted an approach of field monitoring on a landscape consisted of tree and grass covered ground, to investigate the soil temperature effects on root water uptake for a time period from July to November. They found that soil temperature under the grass-covered ground had larger fluctuations and slightly higher values compared to tree-covered
405   ground in summer. (Lozano-Parra et al., 2018) studied the combined effect of soil moisture and vegetation cover on soil temperature over three dryland areas of the Iberian Peninsula for two hydrological years. Under dry conditions, they found smaller daily amplitudes of soil temperature below the tree canopies than in grasslands. (Longobardi et al., 2016) used a global climate model to investigate the climate sensitivity to various rates of deforestation across the globe. According to their results, deforestation warmed the soils of the mid latitudes, because of a reduction in sensible heat fluxes that offset the
410   induced albedo increase. Lastly, (MacDougall and Beltrami, 2017) conducted a GCM experiment to study the historical deforestation impact on subsurface temperatures on global scale. They found that a soil temperature increase remains present for centuries following the deforestation, originated from the reduction of surface energy fluxes towards the atmosphere.

In line with recent findings from observations and model-based studies (Jia et al., 2017; Ren et al., 2018; Zhang et al., 2018; Li et al., 2018), we found that afforestation induced a widespread soil moisture reduction in summer, implying smaller soil
415   heat capacity. This was also a robust feature among the models, albeit with a considerable range in the magnitude of changes. Soil moisture decrease with afforestation resulted from large drying of deep layers, related to the fact that forests and grasslands extract soil water for transpiration process from different soil depths. Furthermore, soil moisture decline determined the increase of summer soil temperature and consequently the increased AAST, in three out of the ten ensemble members, in which the summer GHF sensitivity to afforestation was low. In general, soil moisture changes were not the
420   dominant factor in determining the direction of changes in AAST, moderating only the impact of AAGHF on AAST.

Based on paired observations from FLUXNET dataset, we evaluated the simulated soil temperature response to afforestation. The vast majority of models agreed with the observational evidence that showed a summer ground cooling in forested areas compared to open land. The paired sites exhibited a mean reduction of -3 K in AAST, while the simulated response varied from -5 K to 1 K.

425   The current ensemble enables us to address the role of atmospheric and land processes in the representation of biophysical forcing of land cover change, since it involves simulations which share the same atmospheric model coupled to different land components, or share the same LSM with different atmospheric set-ups. The switch from CCLM to RegCM when both coupled to CLM4.5 did not induce important changes in model results, implying the dominance of land processes in these simulations. Though, among the suite of models which share the NoahMP LSM, the atmospheric configuration selected for
430   WRFb-NoahMP and WRFc-NoahMP significantly refined the afforestation effect on soil temperature, compared to WRFa-NoahMP. Future studies should focus on the evaluation of model performances, similar to (Katragkou et al., 2015), in order to identify the origins of systematic biases and improve the representation of climate processes in simulations. Moreover, our

results stress the crucial role of LSM in the simulation of the biophysical effects of afforestation on soil conditions. Among the land models coupled to the CCLM model, the choice of CLM significantly improves the representation of afforestation impact on AAST. Also, WRF coupled to CLM4.0 agreed better with observations than WRF coupled to NoahMP. Last, problematic behaviours in model performances probably derive from unrealistic descriptions of the physical plant functioning in LSMs. (Meier et al., 2018) improved the representation of the evapotranspiration with land cover change in CLM4.5, modifying parameters related to transpiration process, such as the root distribution and water uptake formulation.

Research has accounted for the contribution of historical deforestation to present climate conditions. Nowadays, governments and non-governmental organizations are planning re/afforestation programs around the world with the purpose to mitigate the negative effects of anthropogenic activities on climate. With our study, we aspire to contribute to the deeper understanding of the scientific community on the biophysical effects of afforestation on soil conditions. Future studies focused on the consequences of afforestation from biological or chemical aspect, are encouraged to consider our results, in order to draw comprehensive conclusions on important climate processes in which afforestation is involved, such as the carbon sequestration and microbial respiration.

Code and data availability

We used soil temperature data from the FLUXNET2015 Tier Two dataset, which can be accessed at the website (https://fluxnet.org/)(last access: 05 March 2021, (Pastorello et al., 2020)). Simulations were forced by the ERA-Interim reanalysis data set (https://www.ecmwf.int/en/forecasts/datasets/reanalysis-datasets/era-interim) (last access:08 March 2021, (Dee et al., 2011). Vegetation maps applied in FOREST and GRASS experiments can be found in (Davin et al., 2020). The source code of the Weather Research and Forecasting Model (WRF) is available by UCAR/NCAR and can be accessed at https://www.mmm.ucar.edu/weather-research-and-forecasting-model (last access: 08 March 2021, (Skamarock et al., 2008)). The documentation of COSMO-Model is available at the following link (https://www.dwd.de/EN/ourservices/cosmo_documentation/cosmo_documentation.html), although a license is required for access (http://www.cosmo-model.org/content/consortium/licencing.htm). RegCM4 model is distributed from https://github.com/ictp-esp/RegCM (last access: 08 March 2021, (Giorgi et al., 2012)). The source code of REMO model is available on request from the Climate Service Center Germany (contact@remo-rcm.de) (Wilhelm et al., 2014). Detailed description on the parameterization schemes and atmospheric settings used from each modelling system can be found in (Davin et al., 2020). All the scripts and data upon which this study is based can be accessed at the link: 10.5281/zenodo.4588724 .

Author contributions

GS and ELD designed the research. GS, EK, ELD, RM, DR, MB, RMC, PH, LJ, PM, PMMS, SS, MHT and KWS performed the RCM simulations. GS analyzed the data and wrote the paper with inputs from all coauthors.

Competing interests.

465   The authors declare that they have no conflict of interest.

References

490 Belušić, D., Fuentes-Franco, R., Strandberg, G., and Jukimenko, A.: Afforestation reduces cyclone intensity and precipitation extremes over Europe, Environ. Res. Lett., 14, 074009, https://doi.org/10.1088/1748-9326/ab23b2, 2019.

Betts, R. A.: Offset of the potential carbon sink from boreal forestation by decreases in surface albedo, Nature, 408, 187–190, https://doi.org/10.1038/35041545, 2000.

Boisier, J. P., Noblet-Ducoudré, N. de, Pitman, A. J., Cruz, F. T., Delire, C., Hurk, B. J. J. M. van den, Molen, M. K. van
495 der, Müller, C., and Voldoire, A.: Attributing the impacts of land-cover changes in temperate regions on surface temperature and heat fluxes to specific causes: Results from the first LUCID set of simulations, 117, https://doi.org/10.1029/2011JD017106, 2012.

Bonan, G. B.: Forests and Climate Change: Forcings, Feedbacks, and the Climate Benefits of Forests, Science, 320, 1444–1449, https://doi.org/10.1126/science.1155121, 2008.

500 Breil, M., Schädler, G., and Laube, N.: An Improved Soil Moisture Parametrization for Regional Climate Simulations in Europe, 123, 7331–7339, https://doi.org/10.1029/2018JD028704, 2018.

Breil, M., Rechid, D., Davin, E. L., Noblet-Ducoudré, N. de, Katragkou, E., Cardoso, R. M., Hoffmann, P., Jach, L. L., Soares, P. M. M., Sofiadis, G., Strada, S., Strandberg, G., Tölle, M. H., and Warrach-Sagi, K.: The Opposing Effects of Reforestation and Afforestation on the Diurnal Temperature Cycle at the Surface and in the Lowest Atmospheric Model
505 Level in the European Summer, 33, 9159–9179, https://doi.org/10.1175/JCLI-D-19-0624.1, 2020.

Broucke, S. V., Luyssaert, S., Davin, E. L., Janssens, I., and Lipzig, N. van: New insights in the capability of climate models to simulate the impact of LUC based on temperature decomposition of paired site observations, 120, 5417–5436, https://doi.org/10.1002/2015JD023095, 2015.

Chen, L., Dirmeyer, P. A., Guo, Z., and Schultz, N. M.: Pairing FLUXNET sites to validate model representations of land-
510 use/land-cover change, 22, 111–125, https://doi.org/10.5194/hess-22-111-2018, 2018.

Cherubini, F., Huang, B., Hu, X., Tölle, M. H., and Strømman, A. H.: Quantifying the climate response to extreme land cover changes in Europe with a regional model, Environ. Res. Lett., 13, 074002, https://doi.org/10.1088/1748-9326/aac794, 2018.

Christensen, J. H. and Christensen, O. B.: A summary of the PRUDENCE model projections of changes in European climate
515 by the end of this century, Climatic Change, 81, 7–30, https://doi.org/10.1007/s10584-006-9210-7, 2007.

Claussen, M., Brovkin, V., and Ganopolski, A.: Biogeophysical versus biogeochemical feedbacks of large-scale land cover change, 28, 1011–1014, https://doi.org/10.1029/2000GL012471, 2001.

Davin, E. L. and de Noblet-Ducoudre, N.: Climatic impact of global-scale Deforestation: Radiative versus nonradiative processes, https://doi.org/10.1175/2009JCLI3102.1, 2010.

520 Davin, E. L., Noblet-Ducoudré, N. de, and Friedlingstein, P.: Impact of land cover change on surface climate: Relevance of the radiative forcing concept, 34, https://doi.org/10.1029/2007GL029678, 2007.

Davin, E. L., Rechid, Di., Breil, M., Cardoso, R. M., Coppola, E., Hoffmann, P., Jach, L. L., Katragkou, E., De Noblet-Ducoudré, N., Radtke, K., Raffa, M., Soares, P. M. M., Sofiadis, G., Strada, S., Strandberg, G., Tölle, M. H., Warrach-Sagi,

K., and Wulfmeyer, V.: Biogeophysical impacts of forestation in Europe: First results from the LUCAS (Land Use and
525 Climate across Scales) regional climate model intercomparison, https://doi.org/10.5194/esd-11-183-2020, 2020.

Dee, D. P., Uppala, S. M., Simmons, A. J., Berrisford, P., Poli, P., Kobayashi, S., Andrae, U., Balmaseda, M. A., Balsamo,
G., Bauer, P., Bechtold, P., Beljaars, A. C. M., Berg, L. van de, Bidlot, J., Bormann, N., Delsol, C., Dragani, R., Fuentes, M.,
Geer, A. J., Haimberger, L., Healy, S. B., Hersbach, H., Hólm, E. V., Isaksen, L., Kållberg, P., Köhler, M., Matricardi, M.,
McNally, A. P., Monge-Sanz, B. M., Morcrette, J.-J., Park, B.-K., Peubey, C., Rosnay, P. de, Tavolato, C., Thépaut, J.-N.,
530 and Vitart, F.: The ERA-Interim reanalysis: configuration and performance of the data assimilation system, 137, 553–597,
https://doi.org/10.1002/qj.828, 2011.

Duveiller, G., Hooker, J., and Cescatti, A.: The mark of vegetation change on Earth's surface energy balance, 9, 679,
https://doi.org/10.1038/s41467-017-02810-8, 2018.

Gálos, B., Hagemann, S., Hänsler, A., Kindermann, G., Rechid, D., Sieck, K., Teichmann, C., and Jacob, D.: Case study for
535 the assessment of the biogeophysical effects of a potential afforestation in Europe, Carbon Balance Manage, 8, 3,
https://doi.org/10.1186/1750-0680-8-3, 2013.

Giorgi, F., Coppola, E., Solmon, F., Mariotti, L., Sylla, M., Bi, X., Elguindi, N., Diro, G., Nair, V., Giuliani, G., Turuncoglu,
U., Cozzini, S., Güttler, I., O'Brien, T., Tawfik, A., Shalaby, A., Zakey, A., Steiner, A., Stordal, F., Sloan, L., and
Brankovic, C.: RegCM4: model description and preliminary tests over multiple CORDEX domains, Clim. Res., 52, 7–29,
540 https://doi.org/10.3354/cr01018, 2012.

Grassi, G., House, J., Dentener, F., Federici, S., den Elzen, M., and Penman, J.: The key role of forests in meeting climate
targets requires science for credible mitigation, 7, 220–226, https://doi.org/10.1038/nclimate3227, 2017.

Hong, S.-Y., Noh, Y., and Dudhia, J.: A New Vertical Diffusion Package with an Explicit Treatment of Entrainment
Processes, 134, 2318–2341, https://doi.org/10.1175/MWR3199.1, 2006.

545 Jacob, D., Teichmann, C., Sobolowski, S., Katragkou, E., Anders, I., Belda, M., Benestad, R., Boberg, F., Buonomo, E.,
Cardoso, R. M., Casanueva, A., Christensen, O. B., Christensen, J. H., Coppola, E., De Cruz, L., Davin, E. L., Dobler, A.,
Domínguez, M., Fealy, R., Fernandez, J., Gaertner, M. A., García-Díez, M., Giorgi, F., Gobiet, A., Goergen, K., Gómez-
Navarro, J. J., Alemán, J. J. G., Gutiérrez, C., Gutiérrez, J. M., Güttler, I., Haensler, A., Halenka, T., Jerez, S., Jiménez-
Guerrero, P., Jones, R. G., Keuler, K., Kjellström, E., Knist, S., Kotlarski, S., Maraun, D., van Meijgaard, E., Mercogliano,
550 P., Montávez, J. P., Navarra, A., Nikulin, G., de Noblet-Ducoudré, N., Panitz, H.-J., Pfeifer, S., Piazza, M., Pichelli, E.,
Pietikäinen, J.-P., Prein, A. F., Preuschmann, S., Rechid, D., Rockel, B., Romera, R., Sánchez, E., Sieck, K., Soares, P. M.
M., Somot, S., Srnec, L., Sørland, S. L., Termonia, P., Truhetz, H., Vautard, R., Warrach-Sagi, K., and Wulfmeyer, V.:
Regional climate downscaling over Europe: perspectives from the EURO-CORDEX community, Reg Environ Change, 20,
51, https://doi.org/10.1007/s10113-020-01606-9, 2020.

555 Jia, X., Shao, M., Zhu, Y., and Luo, Y.: Soil moisture decline due to afforestation across the Loess Plateau, China, Journal of
Hydrology, 546, 113–122, https://doi.org/10.1016/j.jhydrol.2017.01.011, 2017.

Katragkou, E., García-Díez, M., Vautard, R., Sobolowski, S., Zanis, P., Alexandri, G., Cardoso, R. M., Colette, A.,
Fernandez, J., Gobiet, A., Goergen, K., Karacostas, T., Knist, S., Mayer, S., Soares, P. M. M., Pytharoulis, I., Tegoulias, I.,
Tsikerdekis, A., and Jacob, D.: Regional climate hindcast simulations within EURO-CORDEX: evaluation of a WRF multi-
560 physics ensemble, 8, 603–618, https://doi.org/10.5194/gmd-8-603-2015, 2015.

Lawrence, D. M., Fisher, R. A., Koven, C. D., Oleson, K. W., Swenson, S. C., Bonan, G., Collier, N., Ghimire, B.,
Kampenhout, L. van, Kennedy, D., Kluzek, E., Lawrence, P. J., Li, F., Li, H., Lombardozzi, D., Riley, W. J., Sacks, W. J.,
Shi, M., Vertenstein, M., Wieder, W. R., Xu, C., Ali, A. A., Badger, A. M., Bisht, G., Broeke, M. van den, Brunke, M. A.,

Burns, S. P., Buzan, J., Clark, M., Craig, A., Dahlin, K., Drewniak, B., Fisher, J. B., Flanner, M., Fox, A. M., Gentine, P.,
565   Hoffman, F., Keppel-Aleks, G., Knox, R., Kumar, S., Lenaerts, J., Leung, L. R., Lipscomb, W. H., Lu, Y., Pandey, A.,
Pelletier, J. D., Perket, J., Randerson, J. T., Ricciuto, D. M., Sanderson, B. M., Slater, A., Subin, Z. M., Tang, J., Thomas, R.
Q., Martin, M. V., and Zeng, X.: The Community Land Model Version 5: Description of New Features, Benchmarking, and
Impact of Forcing Uncertainty, 11, 4245–4287, https://doi.org/10.1029/2018MS001583, 2019.

Lejeune, Q., Davin, E. L., Guillod, B. P., and Seneviratne, S. I.: Influence of Amazonian deforestation on the future
570   evolution of regional surface fluxes, circulation, surface temperature and precipitation, Clim Dyn, 44, 2769–2786,
https://doi.org/10.1007/s00382-014-2203-8, 2015.

Lejeune, Q., Davin, E. L., Gudmundsson, L., Winckler, J., and Seneviratne, S. I.: Historical deforestation locally increased
the intensity of hot days in northern mid-latitudes, https://doi.org/10.1038/s41558-018-0131-z, 2018.

Li, Y., Zhao, M., Mildrexler, D. J., Motesharrei, S., Mu, Q., Kalnay, E., Zhao, F., Li, S., and Wang, K.: Potential and Actual
575   impacts   of   deforestation   and   afforestation   on   land   surface   temperature,   121,   14,372-14,386,
https://doi.org/10.1002/2016JD024969, 2016.

Li, Y., Piao, S., Li, L. Z. X., Chen, A., Wang, X., Ciais, P., Huang, L., Lian, X., Peng, S., Zeng, Z., Wang, K., and Zhou, L.:
Divergent hydrological response to large-scale afforestation and vegetation greening in China, 4, eaar4182,
https://doi.org/10.1126/sciadv.aar4182, 2018.

580   Longobardi, P., Montenegro, A., Beltrami, H., and Eby, M.: Deforestation Induced Climate Change: Effects of Spatial Scale,
PLOS ONE, 11, e0153357, https://doi.org/10.1371/journal.pone.0153357, 2016.

Lozano-Parra, J., Pulido, M., Lozano-Fondón, C., and Schnabel, S.: How do Soil Moisture and Vegetation Covers Influence
Soil Temperature in Drylands of Mediterranean Regions?, 10, 1747, https://doi.org/10.3390/w10121747, 2018.

MacDougall, A. H. and Beltrami, H.: Impact of deforestation on subsurface temperature profiles: implications for the
585   borehole paleoclimate record, Environ. Res. Lett., 12, 074014, https://doi.org/10.1088/1748-9326/aa7394, 2017.

Meier, R., Davin, E. L., Lejeune, Q., Hauser, M., Li, Y., Martens, B., Schultz, N. M., Sterling, S., and Thiery, W.:
Evaluating   and   improving   the   Community   Land   Model's   sensitivity   to   land   cover,   15,   4731–4757,
https://doi.org/10.5194/bg-15-4731-2018, 2018.

Meier, R., Davin, E. L., Swenson, S. C., Lawrence, D. M., and Schwaab, J.: Biomass heat storage dampens diurnal
590   temperature variations in forests, Environ. Res. Lett., 14, 084026, https://doi.org/10.1088/1748-9326/ab2b4e, 2019.

Ni, J., Cheng, Y., Wang, Q., Ng, C. W. W., and Garg, A.: Effects of vegetation on soil temperature and water content: Field
monitoring and numerical modelling, Journal of Hydrology, 571, 494–502, https://doi.org/10.1016/j.jhydrol.2019.02.009,
2019.

Noblet-Ducoudré, N. de, Boisier, J.-P., Pitman, A., Bonan, G. B., Brovkin, V., Cruz, F., Delire, C., Gayler, V., Hurk, B. J. J.
595   M. van den, Lawrence, P. J., Molen, M. K. van der, Müller, C., Reick, C. H., Strengers, B. J., and Voldoire, A.: Determining
Robust Impacts of Land-Use-Induced Land Cover Changes on Surface Climate over North America and Eurasia: Results
from the First Set of LUCID Experiments, 25, 3261–3281, https://doi.org/10.1175/JCLI-D-11-00338.1, 2012.

Oleson, K., Lawrence, D., Bonan, G., Flanner, M., Kluzek, E., Lawrence, P., Levis, S., Swenson, S., Thornton, P., Dai, A.,
Decker, M., Dickinson, R., Feddema, J., Heald, C., Hoffman, F., Lamarque, J.-F., Mahowald, N., Niu, G.-Y., Qian, T.,
600   Randerson, J., Running, S., Sakaguchi, K., Slater, A., Stockli, R., Wang, A., Yang, Z.-L., Zeng, X., and Zeng, X.: Technical

Description of version 4.0 of the Community Land Model (CLM), UCAR/NCAR, https://doi.org/10.5065/D6FB50WZ, 2010.

Oleson, K., Lawrence, D., Bonan, G., Drewniak, B., Huang, M., Koven, C., Levis, S., Li, F., Riley, W., Subin, Z., Swenson, S., Thornton, P., Bozbiyik, A., Fisher, R., Heald, C., Kluzek, E., Lamarque, J.-F., Lawrence, P., Leung, L., Lipscomb, W.,
605 Muszala, S., Ricciuto, D., Sacks, W., Sun, Y., Tang, J., and Yang, Z.-L.: Technical description of version 4.5 of the Community Land Model (CLM), UCAR/NCAR, https://doi.org/10.5065/D6RR1W7M, 2013.

Pastorello, G., Trotta, C., Canfora, E., Chu, H., Christianson, D., Cheah, Y.-W., Poindexter, C., Chen, J., Elbashandy, A., Humphrey, M., Isaac, P., Polidori, D., Reichstein, M., Ribeca, A., van Ingen, C., Vuichard, N., Zhang, L., Amiro, B., Ammann, C., Arain, M. A., Ardö, J., Arkebauer, T., Arndt, S. K., Arriga, N., Aubinet, M., Aurela, M., Baldocchi, D., Barr,
610 A., Beamesderfer, E., Marchesini, L. B., Bergeron, O., Beringer, J., Bernhofer, C., Berveiller, D., Billesbach, D., Black, T. A., Blanken, P. D., Bohrer, G., Boike, J., Bolstad, P. V., Bonal, D., Bonnefond, J.-M., Bowling, D. R., Bracho, R., Brodeur, J., Brümmer, C., Buchmann, N., Burban, B., Burns, S. P., Buysse, P., Cale, P., Cavagna, M., Cellier, P., Chen, S., Chini, I., Christensen, T. R., Cleverly, J., Collalti, A., Consalvo, C., Cook, B. D., Cook, D., Coursolle, C., Cremonese, E., Curtis, P. S., D'Andrea, E., da Rocha, H., Dai, X., Davis, K. J., Cinti, B. D., Grandcourt, A. de, Ligne, A. D., De Oliveira, R. C.,
615 Delpierre, N., Desai, A. R., Di Bella, C. M., Tommasi, P. di, Dolman, H., Domingo, F., Dong, G., Dore, S., Duce, P., Dufrêne, E., Dunn, A., Dušek, J., Eamus, D., Eichelmann, U., ElKhidir, H. A. M., Eugster, W., Ewenz, C. M., Ewers, B., Famulari, D., Fares, S., Feigenwinter, I., Feitz, A., Fensholt, R., Filippa, G., Fischer, M., Frank, J., Galvagno, M., et al.: The FLUXNET2015 dataset and the ONEFlux processing pipeline for eddy covariance data, 7, 225, https://doi.org/10.1038/s41597-020-0534-3, 2020.

620 Perugini, L., Caporaso, L., Marconi, S., Cescatti, A., Quesada, B., Noblet-Ducoudré, N. de, House, J. I., and Arneth, A.: Biophysical effects on temperature and precipitation due to land cover change, Environ. Res. Lett., 12, 053002, https://doi.org/10.1088/1748-9326/aa6b3f, 2017.

Pitman, A. J., Noblet-Ducoudré, N. de, Cruz, F. T., Davin, E. L., Bonan, G. B., Brovkin, V., Claussen, M., Delire, C., Ganzeveld, L., Gayler, V., Hurk, B. J. J. M. van den, Lawrence, P. J., Molen, M. K. van der, Müller, C., Reick, C. H.,
625 Seneviratne, S. I., Strengers, B. J., and Voldoire, A.: Uncertainties in climate responses to past land cover change: First results from the LUCID intercomparison study, 36, https://doi.org/10.1029/2009GL039076, 2009.

Ren, Z., Li, Z., Liu, X., Li, P., Cheng, S., and Xu, G.: Comparing watershed afforestation and natural revegetation impacts on soil moisture in the semiarid Loess Plateau of China, 8, 2972, https://doi.org/10.1038/s41598-018-21362-5, 2018.

Skamarock, W., Klemp, J., Dudhia, J., Gill, D., Barker, D., Wang, W., Huang, X.-Y., and Duda, M.: A Description of the
630 Advanced Research WRF Version 3, UCAR/NCAR, https://doi.org/10.5065/D68S4MVH, 2008.

Strandberg, G. and Kjellström, E.: Climate Impacts from Afforestation and Deforestation in Europe, 23, 1–27, https://doi.org/10.1175/EI-D-17-0033.1, 2019.

Swenson, S. C., Burns, S. P., and Lawrence, D. M.: The Impact of Biomass Heat Storage on the Canopy Energy Balance and Atmospheric Stability in the Community Land Model, 11, 83–98, https://doi.org/10.1029/2018MS001476, 2019.

635 Tölle, M. H., Breil, M., Radtke, K., and Panitz, H.-J.: Sensitivity of European Temperature to Albedo Parameterization in the Regional Climate Model COSMO-CLM Linked to Extreme Land Use Changes, Front. Environ. Sci., 6, https://doi.org/10.3389/fenvs.2018.00123, 2018.

Wilhelm, C., Rechid, D., and Jacob, D.: Interactive coupling of regional atmosphere with biosphere in the new generation regional climate system model REMO-iMOVE, Geosci. Model Dev., 7, 1093–1114, https://doi.org/10.5194/gmd-7-1093-
640 2014, 2014.

Zhang, S., Yang, D., Yang, Y., Piao, S., Yang, H., Lei, H., and Fu, B.: Excessive Afforestation and Soil Drying on China's Loess Plateau, 123, 923–935, https://doi.org/10.1002/2017JG004038, 2018.